JOURNAL OF VIROLOGY, Jan. 2005, p. 364–379 Vol. 79, No. 1
0022-538X/05/$08.00+0 doi:10.1128/JVI.79.1.364–379.2005

Inverted Terminal Repeat Sequences Are Important for Intermolecular Recombination and Circularization of Adeno-Associated Virus Genomes

Ziying Yan,[1,2] Roman Zak,[1,2] Yulong Zhang,[1,2] and John F. Engelhardt[1,2,3]*

Department of Anatomy and Cell Biology,[1] Department of Internal Medicine,[3] and Center for Gene Therapy,[2] University of Iowa School of Medicine, Iowa City, Iowa

Received 15 April 2004/Accepted 9 September 2004

The relatively small package capacity (less than 5 kb) of adeno-associated virus (AAV) vectors has been effectively doubled with the development of dual-vector heterodimerization approaches. However, the efficiency of such dual-vector systems is limited not only by the extent to which intermolecular recombination occurs between two independent vector genomes, but also by the directional bias required for successful transgene reconstitution following concatemerization. In the present study, we sought to evaluate the mechanisms by which inverted terminal repeat (ITR) sequences mediate intermolecular recombination of AAV genomes, with the goal of engineering more efficient vectors for dual-vector trans-splicing approaches. To this end, we generated a novel AAV hybrid-ITR vector characterized by an AAV-2 and an AAV-5 ITR at opposite ends of the viral genome. This hybrid genome was efficiently packaged into either AAV-2 or AAV-5 capsids to generate infectious virions. Hybrid AV2:5 ITR viruses had a significantly lower capacity to form circular intermediates in infected cells than homologous AV2:2 and AV5:5 ITR vectors despite their similar capacity to express an encoded enhanced green fluorescent protein (EGFP) transgene. To examine whether the divergent ITR sequences contained within hybrid AV2:5 ITR vectors could direct intermolecular recombination in a tail-to-head fashion, we generated two hybrid ITR trans-splicing vectors (AV5:2LacZdonor and AV2:5LacZacceptor). Each delivered one exon of a β-galactosidase minigene flanked by donor or acceptor splice sequences. These hybrid trans-splicing vectors were compared to homologous AV5:5 and AV2:2 trans-splicing vector sets for their ability to reconstitute β-galactosidase gene expression. Results from this comparison demonstrated that hybrid ITR dual-vector sets had a significantly enhanced trans-splicing efficiency (6- to 10-fold, depending on the capsid serotype) compared to homologous ITR vectors. Molecular studies of viral genome structures suggest that hybrid ITR vectors provide more efficient directional recombination due to an increased abundance of linear-form genomes. These studies provide direct evidence for the importance of ITR sequences in directing intermolecular and intramolecular homologous recombination of AAV genomes. The use of hybrid ITR AAV vector genomes provides new strategies to manipulate viral genome conversion products and to direct intermolecular recombination events required for efficient dual-AAV vector reconstitution of the transgene.

Adeno-associated virus (AAV) is a single-stranded DNA parvovirus with a helper-dependent life cycle that replicates in the presence of helper viruses, such as adenovirus or herpesvirus (1, 2). AAV-based vector systems have attracted great attention in the field of human gene therapy for more than 10 years. Although recombinant AAV (rAAV) vectors have now been generated from eight different serotypes (3, 17), type 2 (rAAV-2) has been the most extensively studied as a gene transfer vector. This vector serotype has also been used in clinical trials for cystic fibrosis (14, 36, 37) and hemophilia B (18, 19).

Over the last decade, our knowledge of the molecular virology of rAAV transduction has improved significantly. We now have a better understanding of receptor interactions with AAV, intercellular trafficking, and the conversion of AAV single-stranded DNA viral genomes into transcriptionally active, double-stranded forms (including linear, circular, and concatemer genomes). These studies have led to improvements in the design and performance of rAAV vector systems. For example, genetic modification of AAV capsid proteins and the identification of new AAV serotypes have been applied successfully to overcome cellular barriers to infection caused by limiting receptor abundance (16, 17, 39). Understanding the mechanisms of AAV intracellular trafficking and the involvement of the ubiquitin/proteasome system has led to methods to improve rAAV transduction by enhancing intracellular processing of the virus with proteasome inhibitors (6, 13, 42). In addition, self-complementary or double-stranded AAV vectors have been developed to bypass rate-limiting steps in second-strand synthesis that are required for transgene expression (15, 20, 21, 38).

Studies evaluating the molecular mechanisms of rAAV-2 genome conversion have determined that rAAV genome concatemerization can occur through a process involving intermolecular recombination between two independent linear and/or circular genomes (8, 44). This discovery has led to the development of dual-vector heterodimerization approaches designed to deliver transgene cassettes that exceed the 4.7-kb

* Corresponding author. Mailing address: Department of Anatomy and Cell Biology, University of Iowa Department of Anatomy and Cell Biology, Room 1-111 BSB, 51 Newton Rd., Iowa City, IA 52242-1109. Phone: (319) 335-7753. Fax: (319) 335-7198. E-mail: john-engelhardt@uiowa.edu.

TABLE 1. Viral nomenclature

Proviral plasmid	5′-ITR	3′-ITR	Packaged with AAV-2 capsid	Packaged with AAV-5 capsid
pAV2:2eGFP[a]	AAV-2	AAV-2	AV2:2/2eGFP	AV2:2/5eGFP
pAV5:5eGFP	AAV-5	AAV-5	AV5:5/2eGFP	AV5:5/5eGFP
pAV2:5eGFP	AAV-2	AAV-5	AV2:5/2eGFP	AV2:5/5eGFP
pAV2:2LacZdonor[b]	AAV-2	AAV-2	AV2:2/2LacZdonor	AV2:2/5LacZdonor
pAV2:2LacZacceptor[c]	AAV-2	AAV-2	AV2:2/2LacZacceptor	AV2:2/5LacZacceptor
pAV5:5LacZdonor	AAV-5	AAV-5	NA[d]	AV5:5/5LacZdonor
pAV5:5LacZacceptor	AAV-5	AAV-5	NA	AV5:5/5LacZacceptor
pAV5:2LacZdonor	AAV-5	AAV-2	AV5:2/2LacZdonor	AV5:2/2LacZdonor
pAV2:5LacZacceptor	AAV-2	AAV-5	AV2:5/2LacZacceptor	AV2:5/2LacZacceptor

[a] Previously described as pCisAV.GFP3ori (8).
[b] Previously described as pCisRSVLacZDonor (11).
[c] Previously described as pCisRSVLacZAcceptor (11).
[d] NA, not applicable to this study.

packaging limit of rAAV vectors. This approach uses two independent vectors to deliver separately encoded transgene exons to the same cell with the capability of reconstituting a transgene product by trans-splicing across heterodimer genomes formed by intermolecular recombination (40). Such an approach has effectively doubled the capacity of a single AAV vector and has been tested successfully with reporter genes in muscle (12, 35, 43), liver (26), and eyes (29). Since the 4.7-kb packaging capacity limits the application of rAAV for diseases such as cystic fibrosis, Duchenne muscular dystrophy, and hemophilia A, dual-vector approaches may be useful in the application of rAAV for such disease genes.

Despite the promising prospects of dual rAAV vector approaches, the level of gene expression from the current system remains substantially lower than delivery of a transgene encoded within a single vector. Several factors currently limit the efficiency of dual-vector heterodimerization approaches. First, the multiplicity of infection must be high enough to ensure the probability that both delivered vectors infect and recombine in the same cell. Second, in the context of dual-vector, trans-splicing approaches, the reconstitution of a functional transgene is directionally dependent on the union of two viral genomes in the correct orientation. For dual vectors containing two minigene exons in the same orientation, only heterodimers formed by a tail-to-head recombination event are active to trans-splice a functional reconstituted transgene. In this context, approaches aimed at increasing the ratio of tail-to-head-oriented heterodimers and larger concatemers could conceivably improve the efficiency of dual-vector trans-splicing delivery of transgene products. However, the mechanisms responsible for intermolecular recombination of rAAV genomes are poorly understood.

Our previous studies in muscle have suggested that monomer circular viral genome intermediates, with a double-D inverted terminal repeat (ITR) structure, may be precursors to the formation of episomally stable concatemers (8, 43). In these studies, intermolecular recombination appears to occur between monomer circular genomes in a time-dependent manner, leading to high-molecular-weight circular concatemers. In contrast, studies in the liver with rAAV and linear AAV-like genomes have suggested that concatemerization may be independent of the ITR and primarily involve linear intermolecular end-end ligation (24, 25, 27). A clear delineation of these two mechanisms as well as potential tissue-specific differences is critical to improve the efficiency of rAAV dual-vector approaches.

Engineering dual-vector sets with a preferred recombinational bias to form tail-to-head heterodimers is one possible way to overcome the limitation of random recombination that reduced trans-splicing efficiency. Fundamental to such a strategy is a clear delineation of ITR involvement in the recombination process. To approach these questions, we used two of the most divergent (less than 50% conserved) ITR sequences derived from AAV-2 and AAV-5 to generate a novel hybrid ITR vector genome. This hybrid ITR viral vector contained one AAV-2 ITR and one AAV-5 ITR at opposite ends of the viral genome. Hybrid ITR vectors functionally transduced a single encoded transgene at an efficiency similar to that of the native rAAV-2 or rAAV-5 vectors that have homogeneous ITRs on both ends.

We used these AAV-2:5 ITR hybrid viruses as a means to study the involvement of ITR sequences in genome circularization and concatemerization resulting from viral DNA intra- and intermolecular recombination. The ability of hybrid ITR vectors to form circular intermediates was evaluated by Hirt Southern blots and a bacterial rescue assay. Hybrid ITR vectors demonstrated a reduced ability to form monomer circular intermediates. They also showed an increased efficiency for directional tail-to-head intermolecular recombination of linear genomes capable of expressing a dual-vector-encoded trans-spliced gene product. These results suggest that ITR-mediated recombination events are critical for AAV genome circularization and concatemerization. Altering the ITR sequence to facilitate directional homologous recombination between independent vector genomes is therefore a useful approach to enhance dual-vector gene delivery.

MATERIALS AND METHODS

Recombinant virus and proviral plasmid nomenclature. In total, nine viral vectors with various combinations of AAV-2 and/or AAV-5 ITRs and capsids were evaluated in this study. For clarity of presentation, we have standardized the nomenclature of various recombinant virus particles, genomes, and proviral plasmids, as outlined in Table 1. In general, pAVa:bTransgene denotes the proviral plasmids used to generate a virus, where a and b represent the 5′ and 3′ ITRs in relationship to the reading frame of the encoded transgene, respectively. AVa:bTransgene refers to the viral DNA packaged into the viral capsid. AVa:b/cTransgene refers to the intact recombinant virus particle, where c indicates

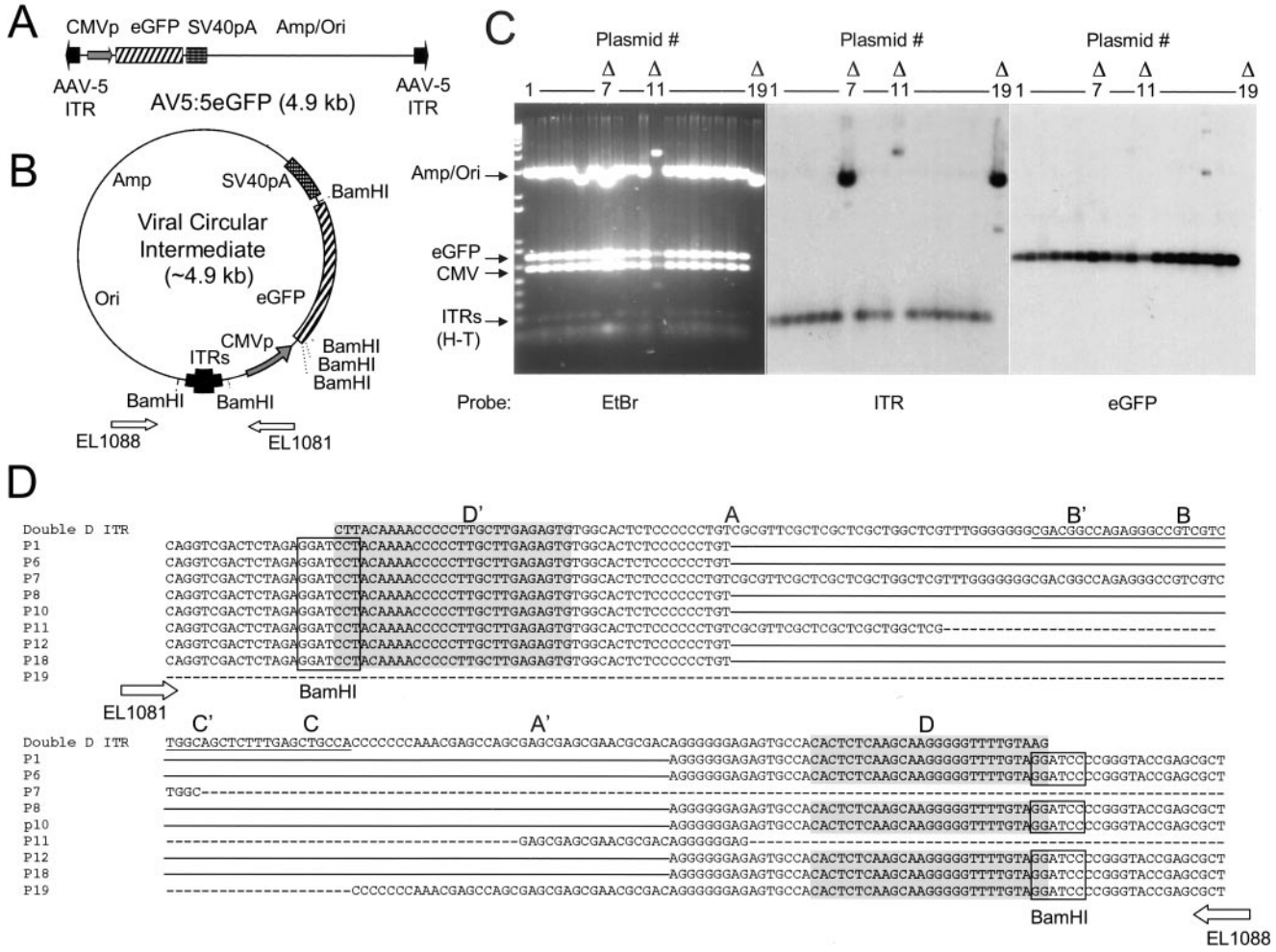

FIG. 1. Characterization of circular AV5:5/5 vector genomes. To evaluate the ability of the AV5:5/5 virus to form circular intermediates, we used an EGFP shuttle vector to rescue replication-competent plasmids from bacteria following transformation with Hirt DNA from AV5:5/5eGFP-infected HeLa cells (500 DNase-resistant particles/cell). (A) Schematic diagram of the AV5:5eGFP viral genome. (B) The predominant form of rescued circular rAAV-5 intermediates is represented as a double-D circular monomer. The positions of the BamHI sites used for restriction mapping and the primers (EL1080 and EL1088) used for sequencing of the double-D ITR junction are shown. (C) Restriction enzyme and Southern blotting analyses of rescued AV5:5eGFP circular intermediates are displayed. Plasmids from 19 randomly chosen colonies were analyzed by BamHI digestion, followed by Southern blotting with ^{32}P-labeled AAV-5 ITR and EGFP probes. The major bands of BamHI digestion from an AV5:5eGFP double-D circular monomer are expected to migrate as a ≈200-bp double-D ITR fragment, a 620-bp cytomegalovirus promoter fragment, a 760-bp EGFP cDNA fragment, and a ≈3-kb band containing the simian virus 40 polyadenylation site and the ampicillin resistance and *ori* sequences. Isolated clones incurring deletions (Δ) within the ITR junction are marked above the gel. (D) The sequence of ITR junctions from AV5:5eGFP circular intermediates is shown in panel C. The EL1081 (5′-CAAGTGGGCAGTTTACCGTA-3′) and EL1088 (5′-CATTAATGCAGCTGGCACGA-3′) primers were used for sequencing the AAV-5 ITR junction as positioned in panel B. The sequence results from individual rescued circular intermediates are aligned against a predicted double-D AAV-5 head-to-tail ITR junction. BamHI sites in the sequence are marked with a box. Known deletions confirmed by sequencing are marked with dashed lines, and regions that could not be sequenced due to secondary structure are marked with solid lines. Sequences from all other clones not shown were identical to p1.

the capsid serotype. In the present study, a and b ITRs and c capsids were of AAV-2 or AAV-5 origin.

AAV-5 ITR cloning. A 167-bp AAV-5 ITR with EcoRI and XhoI sites flanking the 5′ A sequence and a BamHI site at the 3′ end of the D sequence was synthesized by IDT, Inc. (Coralville, Iowa) according to the previously published AAV-5 sequence (5). The synthetic fragment was cloned into the BamHI and EcoRI sites of pUC19 to give the plasmid intermediate pUC.AV5ITR. A second intermediate cloning vector was pITR.5R/2L, which contained both the AAV-2 and AAV-5 ITRs at the right and left ends of the viral genome, respectively, separated by a portion of the luciferase cDNA. With BamHI and XhoI double digestion, pITR.5R:2L was generated from an AAV-2 proviral plasmid, pCis.AV2.ampicillin resistance/ori, by replacing one AAV-2 ITR with the AAV-5 ITR from pUC.AV5ITR. The AAV-5 ITR sequence in pUC.AV5ITR and pITR.5R:2L was confirmed by a dideoxy thermocycling sequencing procedure conducted through the DNA facility at the University of Iowa. In order to eliminate the secondary structure of the ITR and to allow complete sequence reading, the AAV-5 ITR-containing plasmids were digested by EaeI prior to sequencing, which linearized the ITR at the junction of the A sequence and the B-C loop. The integrity of the AAV-5 ITR in subsequent cloning processes was confirmed by enzymatic digestion with the EaeI diagnostic assay and other restriction enzymes flanking the ITR (such as BamHI and XhoI).

Construction of rAAV-5 and rAAV-2:5 ITR hybrid proviral plasmid. The nomenclature for various proviral plasmids and viruses is included in Table 1. A 1.4-kb AflIII/XbaI (blunted) fragment containing an AAV-5 ITR and a portion of the stuffer sequence from pITR.5R:2L was inserted into pUC.AV5ITR to form the AAV-5 proviral plasmid pAV5:5amp/ori. An en-

hanced green fluorescent protein (EGFP) expression cassette from pAV2:2eGFP (previously described as pCisAV.GFP.3ori) (8) was then inserted into a PstI site to generate pAV5:5eGFP. The hybrid ITR proviral plasmid pAV2:5eGFP featured an EGFP expression cassette flanked by an AAV-2 and AAV-5 ITR at both ends. This vector was generated by inserting the BglII/SalI (blunted) fragment from pAV2:2eGFP (which contained one AAV-2 ITR and the EGFP cassette) into the BglII and AflIII (blunted) sites of pAV5:5amp/ori. BglII and AflIII digestion of pAV5:5amp/ori removed one AAV-5 ITR and 380 bp of adjacent linker sequence (hence, the AV2:5 vector genome is slightly shorter than AV2:2 or AV5:5). pAV2:2eGFP, pAV5:5eGFP, and pAV2:5eGFP all harbor an EGFP expression cassette, an ampicillin resistance gene, and an *Escherichia coli* replicon in the AAV proviral genome. They have identical genomic organizations with the exception of the ITR sequences. pAV2:2eGFP was previously used to generate the rAAV-2 shuttle virus AV2:2/2eGFP, which is capable of isolating circular viral genomes from Hirt DNA by bacterial transformation (8, 44).

β-Galactosidase trans-splicing vectors. Three rAAV-2 β-galactosidase trans-splicing dual-vector sets were generated with AAV-2, AAV-5, and AAV-2:5 hybrid ITRs to evaluate ITR-mediated intermolecular recombination (Table 1). Type 2 ITR-based vectors were generated from two proviral plasmids, pAV2:2LacZdonor and pAV2:2LacZacceptor (previously described as the pCisLacZDonor and pCisLacZAcceptor, respectively) (11). These two plasmids were used to generate the AAV-2-based trans-splicing viruses AV2:2LacZdonor and AV2:2LacZacceptor. In brief, these vectors each contain half of a Rous sarcoma virus enhancer/promoter-driven β-galactosidase expression cassette. The promoter, the 5′ half of the *lacZ* gene, and a splicing donor consensus sequence were cloned in the donor proviral plasmid pAV2:2LacZdonor. The backbone of the donor plasmid was from pSub201 (30). The acceptor vector was obtained by replacing the EGFP cassette in pAV2:2eGFP with a splice acceptor sequence, the remainder of the 3′ portion of the *lacZ* gene, and a simian virus 40 polyadenylation site.

Through a series of subcloning steps, the AAV-2 ITR in pAV2:2LacZdonor and pAV2:2LacZacceptor was replaced with the AAV-5 ITR without the transgene cassettes being altered, generating the AAV-5-based trans-splicing proviral plasmids pAV5:5LacZdonor and pAV5:5LacZacceptor, respectively. These proviral plasmids were used to generate rAAV-5-based trans-splicing viruses, which were called AV5:5LacZdonor and AV5:5LacZacceptor, respectively. The AAV-2:5 hybrid ITR vector set was generated from the donor plasmid pAV5:2LacZ donor, and the acceptor plasmid was generated from pAV2:5LacZacceptor.

To construct pAV5:2LacZdonor, both pAV2:2LacZdonor and pAV5:5LacZ donor were digested with XmnI and SphI. The 2.5-kb fragment from pAV5:5LacZdonor that contained the AAV-5 ITR and a portion of the Rous sarcoma virus promoter was then cloned into the XmnI- and SphI-digested backbone of pAV2:2LacZdonor in order to generate pAV5:2LacZdonor. This proviral plasmid contained the AAV-5 and AAV-2 ITRs on the 5′ and 3′ ends of the transgene cassette, respectively (the 5′ end is denoted as the ITR most proximal to the 5′ end of the inserted reading frame). The pAV2:5LacZacceptor proviral vector was cloned by a fragment exchange between pAV2:2LacZacceptor and pAV5:5LacZacceptor. In order to generate the pAV2:5LacZacceptor vector, the 2.3-kb NotI/BglII (blunted) fragment from pAV5:5LacZacceptor containing the partial stuffer sequence and the AAV-5 ITR linked to the splicing acceptor was replaced with the 2.6-kb NotI/XbaI (blunted) fragment derived from pAV2:2LacZacceptor containing the AAV-2 ITR.

Recombinant AAV vector production and purification. Table 1 depict the nomenclature used to systematically describe the various viral vectors and proviral plasmids used in this study. Since the present study sought to compare both type 2 and type 5 capsid viruses, we chose a standard method of purification with double-banded CsCl isopycnic centrifugation for all viral production methods. A routine calcium phosphate cotransfection protocol was used to produce rAAV from 293 cells (40), with the exception that an adenoviral helper plasmid, pAd4.1 (property of Targeted Genetics), was used in the cotransfection cocktail. In order to produce the rAAV-2 or rAAV-5 virus, the cotransfection protocol included the rAAV-2 proviral plasmid pAV2RepCap and pAd4.1 or the AAV-5 proviral plasmid pAV5RepCap and pAd4.1 at a mass ratio of 1:3:3. Protocols similar to those described previously were used to pseudotype rAAV-2 genomes into AAV-5 capsids and rAAV-5 genomes into AAV-2 capsids (41).

These protocols were also used to package the hybrid ITR vectors. The hybrid ITR virus was packaged with the AAV-2 capsid by transfecting the pAV2:5ITR or pAV5:2ITR proviral constructs into 293 cells together with pRep5, pAV2RepCap, and pAd4.1 at a mass ratio of 1:1:3:3. Hybrid ITR viruses with the AAV-5 capsid were generated by cotransfection of the pAV2:5ITR or pAV5:2ITR proviral plasmid with pRep2, pAV5RepCap, and pAd4.1 at a mass ratio of 1:1:3:3. Cells were harvested 70 h after transfection, and virus particles were released by freeze-thawing, DNase I digestion, and deoxycholate treatment, as previously described (41). All viral stocks were purified with the same CsCl ultracentrifugation procedure. Following two rounds of CsCl banding, the fractions of 1.36 to 1.42 g/cm^3 were collected. After dialysis against HEPES-buffered saline at 4°C to remove the CsCl, the viral stocks were quantified by slot blot.

The integrity of packaged viral genomes was evaluated by slot blot hybridization assays of viral DNA. The probes used for this analysis included flanking sequences outside the AAV-2 or AAV-5 ITR (i.e., in the proviral backbone stuffer sequence, a portion of the luciferase cDNA) as well as specific probes against the AAV-2 ITR, AAV-5 ITR, and EGFP gene. Unless otherwise specified in the figure legends, all probes were generated with a random primer-labeling method with plasmid-derived DNA fragments of AAV-2, AAV-5, EGFP, or luciferase as the template. Typical, activities of the probes were approximately 400,000 to 800,000 cpm/μl. The hybridizations were performed at a probe concentration of 10^6 cpm/ml (hybridization buffer). Viral DNAs were also evaluated in alkaline-denaturing agarose gels (1% [wt/vol] agarose in 50 mM NaOH, 1 mM EDTA solution), followed by Southern blotting with a ^{32}P-labeled EGFP probe.

Virus infection and evaluation of transgene expression. HeLa cells or ferret fetal primary fibroblasts were cultured as monolayers in Dulbecco's modified Eagle's medium (DMEM) and then supplemented with 10% fetal bovine serum (HyClone Laboratories, Inc), 100 U of penicillin per ml, and 100 μg of streptomycin per ml. They were maintained in a 37°C incubator at 5% CO_2. Cells were seeded at a density of 5×10^5 cells per six-well plate or 2×10^5 cells per 12-well plate 1 day before infection. Immediately prior to infection, cells were washed once with DMEM supplemented with 0% serum. The virus was then mixed with serum-free DMEM and applied directly to cells. At 1 h postinfection, an equal amount of DMEM–20% fetal bovine serum was added to each culture, bringing the final serum content to 10%.

For evaluation of EGFP-expressing vectors, AV2:2/2eGFP, AV5:5/5eGFP, AV2:5/2eGFP, and AV2:5/5eGFP were used to infect HeLa cells cultured in six-well plates at a multiplicity of infection of 500 DNase-resistant particles per cell. At 24 h postinfection, EGFP expression was analyzed by indirect fluorescence microscopy. Cells were collected for extraction of low-molecular-weight DNA by a modified Hirt method, as previously described (40).

Evaluation of *lacZ* trans-splicing expression of β-galactosidase was performed on HeLa cells or primary fetal fibroblasts seeded at 5×10^5 cells per six-well plate or 2×10^5 cells per 12-well plate. Six-well cultures were used for 5-bromo-4-chloro-3-indolyl-β-D-galactopyranoside (X-Gal) histochemical staining and Hirt DNA extraction, while 12-well cultures were used for enzymatic assays. Viral infections were performed on 70% confluent HeLa cells or 90% confluent fibroblast cultures as described above, with a multiplicity of infection of 2.5×10^3 DNase-resistant particles per cell for each virus. Transgene expression assays were performed at 72 h postinfection. The β-galactosidase expression from trans-splicing vector-infected cells was evaluated by in situ X-Gal staining and/or enzymatic assay with a Galacto-Light Plus system (Applied Biosystems, Bedford, Mass.), as previously described (11). For the enzymatic assay, the cell lysate supernatant was heated at 48°C for 1 h to inactivate the endogenous β-galactosidase activity.

Rescue of circular viral genomes from AAV-transduced cells. Low-molecular-weight DNA was extracted from AAV-infected cells, as previously reported (40, 43). For each experimental point, the final DNA pellet from one well of the six-well plate culture was dissolved in 50 μl of H_2O, and one-tenth of the total volume (5 ul) was used to transform *E. coli* Sure cells [e14$^-$ (McrA$^-$) Δ(*mcrCB-hsdSMR-mrr*)*171 endA1 supE44 thi-1 gyrA96 relA1 lac recB recJ sbcC umuC*::Tn*5* (Kan^r) *uvrC* [F′ *proAB lacI*^{q}ZΔ (M15 Tn*10* (Tet^r))]] by electroporation. The resultant ampicillin-resistant colonies were quantified, and a portion of the rescued plasmids were used for molecular analysis by restriction enzymes, Southern blotting, and sequencing with a dideoxy thermocycling sequencing procedure.

RESULTS

rAAV-5 forms circular intermediates and heterodimers in HeLa cells and fetal fibroblasts. Despite the wide body of knowledge elucidating the transduction biology of rAAV-2 vectors, little is known about the similarities and differences between the viral processing events of rAAV-2 and other vector serotypes. Among all the cloned AAV genomes, AAV-5 is the most distinct member in terms of genome sequence and tropism. Detailed sequence comparisons between the AAV-2

and AAV-5 genomes indicate a large diversity in the sequences of the capsid and Rep proteins and their ITR structures. Although the AAV-2 and AAV-5 ITRs show less than 50% homology in nucleotide sequence, the predicted secondary structures of these two palindromic sequences have similar stem-loop hairpin conformations. Despite the fact that the Rep protein-binding motifs of AAV-2 and AAV-5 ITRs are highly conserved, it has been reported that AAV-5 and AAV-2 Rep78 proteins cannot cleave the terminal resolution site (*trs*) at the AAV-2 and AAV-5 ITRs (4). This is thought to be the reason AAV-2 and AAV-5 Rep proteins cannot cross-complement virus replication (5).

Since AAV ITRs contain all the necessary *cis*-functions required for virus replication, it is very possible that the mechanisms of DNA strand conversion may be similar between these two serotypes despite primary ITR sequence divergence. Previously, our group and others have described conversion productions of rAAV-2 genomes that involve the formation of episomal circular monomer or concatemer genomes (8, 23, 33, 34). However, it is currently unclear whether rAAV-5 undergoes similar molecular processes of genome conversion. To address this question, we first constructed an rAAV-5 shuttle virus (AV5:5/5eGFP) to test whether the rAAV-5 genomes also form circular transduction intermediates. This AV5:5/5eGFP vector contained the EGFP reporter and an *E. coli* replicon/ampicillin resistance gene between two AAV-5 ITRs and D sequences (Fig. 1A). The ampicillin resistance gene and *E. coli* replicon facilitated the rescue and amplification of circular transduction intermediates by transforming Hirt DNA harvested from infected cells into bacteria.

Studies with this rescue assay in AV5:5/5eGFP-infected HeLa cells have demonstrated that 320 ± 8 ($n = 4$) CFU can be rescued on agar plates containing ampicillin. Although the total number of rescued circular intermediates was approximately 11-fold lower than that obtained from AV2:2/2eGFP infection ($3{,}488 \pm 208$ CFU), this is to be expected because rAAV-5 capsid-mediated transduction in HeLa cells is approximately fivefold less efficient than transduction mediated by the rAAV-2 capsid (41). Previously, we reported that self-circularization of monomer genomes in a head-to-tail fashion occurs following rAAV-2 infection. Sequencing analysis of rescued circular genomes demonstrated a predominant double-D ITR structure (D′-A-B′-B-C′-C-A′-D) at the head-to-tail junction of these intermediates (7, 9).

We hypothesize that if the mechanism of rAAV-5 genome conversion were similar to that of rAAV-2, AAV-5 circular monomer genomes would assume the structure depicted in Fig. 1B. Structural analysis of rAAV-5 circular intermediates was performed with BamHI digestion. Such digestion was expected to give an approximately 200-bp fragment for the double-D ITR junction, a 620-bp fragment for the cytomegalovirus promoter segment, a 760-bp fragment for the EGFP cDNA, and a large 3-kb band containing the simian virus 40 polyadenylation site and ampicillin resistance and *ori* sequences. We randomly isolated 19 ampicillin-resistant colonies to evaluate the structure of rAAV-5 circular intermediates. The plasmids from these colonies were then evaluated by BamHI digestion followed by Southern blot hybridization with EGFP and AAV-5 ITR probes. The result of this analysis is shown in Fig. 1C.

We found that the uniform BamHI digestion pattern of most of the plasmids tested was very similar to that observed previously for AV2:2eGFP (with PstI and SphI digestion) (8); 16 of the 19 clones tested (84%) matched the predicted BamHI restriction map and Southern blot profile of a monomer double-D AV5:5eGFP circular genome (Fig. 1C). Two of the clones (p5 and p7) had an approximately 200- to 300-bp internal deletion in the ampicillin resistance-*ori* fragment. Three of the clones (p7, p11, and p19) lacked a 200-bp ITR fragment but had a larger AAV-5 ITR-hybridizing band. In addition, deletion of the EGFP gene and the cytomegalovirus promoter also occurred in p19. Such deletions surrounding the ITR junction were also observed at low frequencies in AV2:2eGFP circular intermediates (8).

To evaluate the ITR junction of rAAV-5 circular intermediates in more detail, all 19 plasmids were sequenced with primers (EL1080 and EL1088) that flanked the 5′ ITR and the 3′ ITR, respectively. Although complete sequencing across the ITR junction was not possible due to limited restriction enzyme sites in the AAV5 ITR needed to reduce secondary structure, these studies did confirm ITR deletions found in 3 of the 19 clones (Fig. 1D). It is unclear whether these deletions occurred in vivo during the circularization process or during the genome rescue process in *E. coli*. The remaining 16 plasmids were accessible to sequencing by the EL1081 and EL1088 primers. However, due to the strong secondary structure of the ITR junction region, we could not obtain the full ITR sequence of these clones; the sequencing prematurely terminated at a similar position in all clones at the A or A′ sequence. Based on the findings that a 200-bp ITR-hybridizing band was released by BamHI digestion from these plasmids and the sequence confirmed intact D and D′ sequences at the ITR junction, we predict the double-D junction of AAV-5 circular intermediates (D-A′-B-B′-C-C′-A-D′) to be similar to that previously described for AAV-2-based vectors (8, 43, 44). Additionally, the variability in the integrity of the AAV-5 ITR junctional sequences also appears to be similar to that previously described for rAAV-2 (9, 44).

To evaluate the extent to which rAAV-5 genomes undergo intermolecular recombination, we used a dual-vector heterodimerization approach that reconstitutes β-galactosidase expression by trans-splicing between two independent vector genomes, each harboring an exon of the *lacZ* minigene. To this end, we constructed two *lacZ* trans-splicing vectors (AV5:5/5LacZdonor and AV5:5/5LacZacceptor, Fig. 2A). Each harbored the AAV-5 ITR at both ends of the viral genome. As previously observed for rAAV-2 trans-splicing vectors (43), reconstitution of β-galactosidase expression was seen only in fetal fibroblasts coinfected with AV5:5/5LacZdonor and AV5:5/5LacZacceptor (Fig. 2B) and not in fibroblasts infected with only one of the two vectors. These findings demonstrate that rAAV-5 genomes are capable of forming heterodimers through intermolecular recombination. The level of reconstituted β-galactosidase expression was low in these studies because the level of AAV-5 capsid transduction in primary fibroblasts is approximately 10-fold lower than that for AAV-2 capsid vectors.

To directly evaluate whether the AAV-2 and AAV-5 ITRs have similar capacities for intermolecular recombination, we also compared the ability of AAV-2 and AAV-5 ITR vector

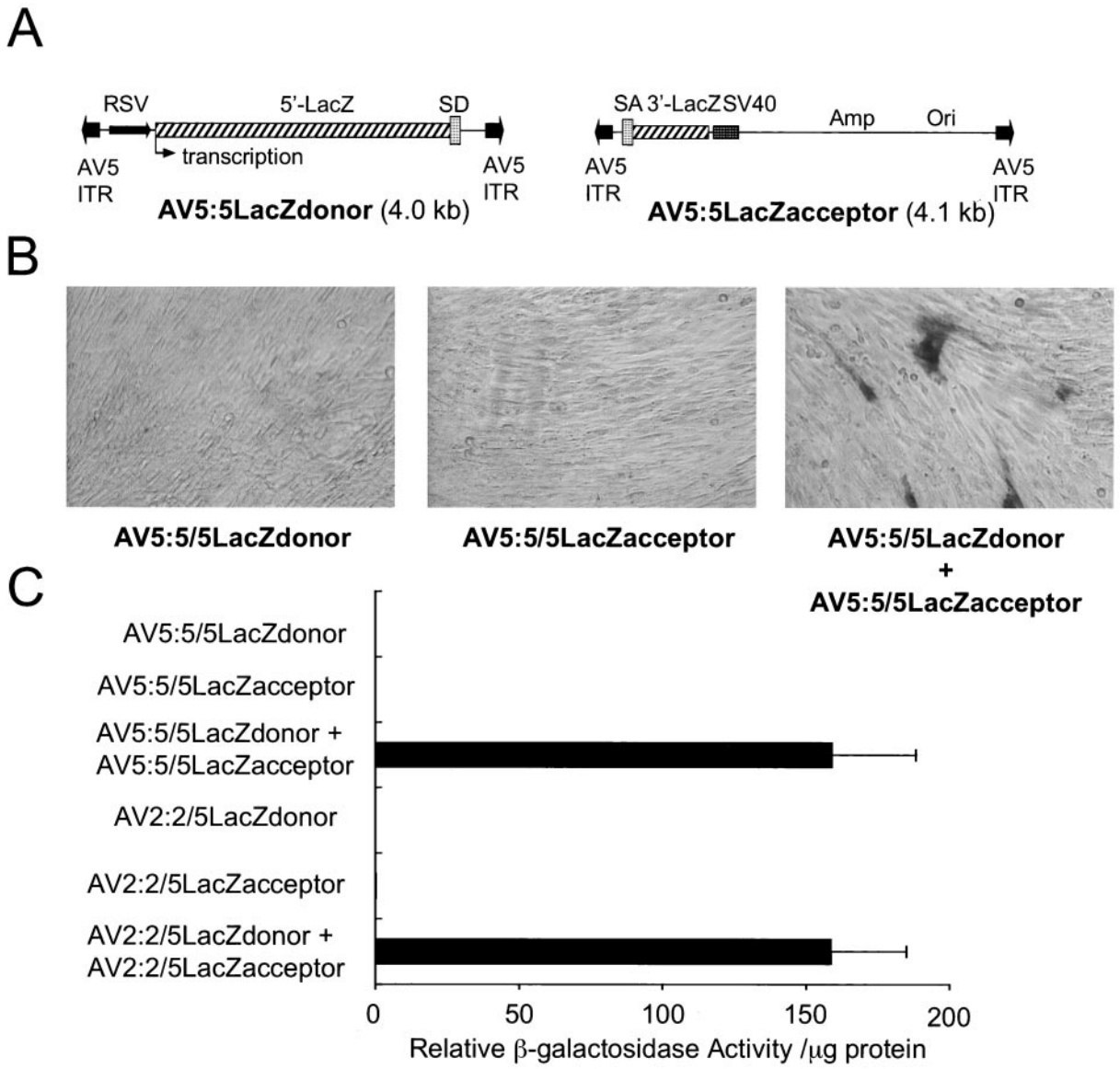

FIG. 2. Dual rAAV vector reconstitution of a β-galactosidase minigene through heterodimerization with the AV2:2 or AV5:5 vector. (A) Schematic representation of the rAAV-5-based *lacZ* trans-splicing vectors used to assess heterodimerization. Only heterodimerization of these two vectors in a tail-to-head orientation is capable of reconstituting a functional *lacZ* gene product. 5′-LacZ, the first half of the *lacZ* genome; 3′-LacZ, the second half of the *lacZ* genome; SD, splice donor; SA, splice acceptor; RSV, promoter/enhancer; SV40, polyadenylation sequences; Amp, ampicillin resistance gene; Ori, bacterial replication origin. (B) Ferret fetal fibroblasts were coinfected with the AV5:5/5LacZdonor or AV5:5/5LacZacceptor virus at a multiplicity of infection of 2,500 DNase-resistant particles/cell. Cells were then functionally evaluated for β-galactosidase expression by histochemical X-Gal staining at 7 days postinfection. (C) The efficiency of heterodimerization for AV2:2 and AV5:5 vector genomes were compared in HeLa cells with dual-vector trans-splicing reconstitution of β-galactosidase expression. All viruses were packaged into AAV-5 capsids. HeLa cells were infected at a multiplicity of infection of 2,500 DNase-resistant particles/cell with each virus alone or in combination, as indicated. β-Galactosidase activity was quantified at 3 days postinfection. Data represent the mean (± standard error of the mean) of four independent infections.

genomes to reconstitute dual-vector-based transgene expression. To avoid capsid tropism effects on the level of transduction, both AV2:2 and AV5:5 donor and acceptor genomes were packaged into AAV-5 capsids for the comparison. The results from these experiments in HeLa cells (Fig. 2C) demonstrated indistinguishable reconstitution of β-galactosidase transgene expression following coinfection with AV2:2/5donor plus AV2:2/5acceptor or AV5:5/5donor plus AV5:5/5acceptor vector combination. No β-galactosidase expression was seen following infection with any of the vectors alone. Since reconstitution of β-galactosidase expression can only be obtained following head-to-tail intermolecular recombination, these results demonstrate that rAAV-2 and rAAV-5 ITRs have similar capacities for recombination.

AV2:5 hybrid ITR vector genomes can efficiently package into AAV-2 or AAV-5 capsids to assemble infectious virions.

Molecular analyses of episomal rAAV intermediates have revealed that a head-to-tail double-D ITR structure is the most common type of circular intermediate rescued following both rAAV-2:2 and rAAV-5:5 transduction. However, sequence analysis of double-D intermediates has demonstrated that approximately 15% of isolated circular intermediates contain genetic information from more than one but fewer than two ITRs at the head-to-tail double-D junction (9). Two explanations may account for this heterogeneity in the ITR junctions of circular intermediates. First, circularization may occur through nonspecific intramolecular end-end ligation, followed by recombination events in bacteria that reduce the ITR to a more stable double-D structure. In support of this hypothesis, end-end joining of viral genomes has been proposed by others to be responsible for the formation of intramolecular linear concatemers (25, 27). Second, intramolecular circularization of viral genomes might occur through ITR-mediated homologous recombination, as previously proposed (9). If this process of homologous recombination is not exact, as might be expected because flip-and-flop hairpin loops exist in equal proportions in the viral genome, this could also explain the heterogeneity in the ITR junctional sequence found in circular AAV genomes.

To distinguish between these two possibilities, we have generated hybrid ITR vectors harboring an AAV-2 and AAV-5 ITR at either end of the viral genome. As AAV-2 and AAV-5 ITR show less than 50% homology in their sequences (Fig. 3A), we hypothesized that if homologous recombination were the predominant mechanism of rAAV genome circularization, such hybrid vectors would be impaired in this process. However, for such experiments to be informative, it was first necessary to confirm that hybrid ITR AAV genomes could effectively produce infectious viruses. To this end, we developed methods for packaging pAV2:5eGFP genomes (Fig. 3B) into both AAV-2 and AAV-5 capsids to generate progeny viruses AV2:5/2eGFP and AV2:5/5eGFP, respectively.

Similar to pseudotyping AAV-2 genomes with AAV-5 capsids, both Rep5 and Rep2 were required for packaging the pAV2:5eGFP genome into either AAV-2 or AAV-5 capsids. The yield of the hybrid viruses, AV2:5/2eGFP and AV2:5/5eGFP, was typically only one- to twofold lower than that seen with AV2:2/2eGFP and AV5:5/5eGFP vectors containing homologous AAV-2 or AAV-5 ITRs at either end of the genome. To confirm the packaging of the intact hybrid ITR viral genome, 10^9 particles of AV2:2/2eGFP, AV2:5/2eGFP, and AV5:5/5eGFP were digested with proteinase K. Viral DNAs were subsequently resolved in an alkaline-denaturing agarose gel and then visualized by probing Southern blots with a ^{32}P labeled EGFP probe. The apparent migration positions of the hybridizing viral genomes (Fig. 3C) corresponded to the predicted sizes of full-length linear viral genomes (AV2:5/5eGFP, 4.4 kb; AV2:2/2eGFP, 4.8 kb; and AV5:5/2eGFP, 4.9 kb). These results confirmed that effective viral replication was initiated from the hybrid ITR proviral plasmid and that intact hybrid ITR genomes could be efficiently replicated and packaged into viral particles.

The packaging of intact vector genomes was further confirmed by a series of slot blot hybridization experiments with viral DNA from purified AV2:5/2eGFP, AV2:5/5eGFP, AV2:2/2eGFP, and AV5:5/5eGFP viruses (Fig. 3D). Probes used for this analysis included DNA flanking sequences outside the AAV-2 or AAV-5 ITR (i.e., in the proviral backbone stuffer sequence, a portion of the luciferase cDNA) as well as specific probes against the AAV-2 ITR, AAV-5 ITR, and EGFP gene. Hybridization of viral DNA with stuffer sequence probes demonstrated approximately 10% of the viral genomes contained such sequences when compared to an EGFP probe. This was similar for both rAAV-2 and rAAV-5 packaged virions regardless of their ITR structure. This type of stuffer sequence packaging is also typical for rAAV vector production (22, 28). Importantly, the ratio of ITR to EGFP hybridization demonstrated that both AAV-2 and AAV-5 ITRs were efficiently packaged into AV2:5/5 and AV2:5/2 virions.

Since both AAV-2 and AAV-5 Rep proteins are required for the production of hybrid ITR viruses, there remained a possibility that AV2 or AV5 Rep proteins might have different nicking efficiencies that could lead to a preference for minus- or plus-strand genome packaging. Similarly, interactions between each Rep78 protein serotype and a given capsid serotype might also affect strand-packaging preference. To this end, we evaluated the polarity of packaged hybrid ITR vector genomes by slot blot with ^{32}P-labeled oligonucleotide probes specific to either the sense or antisense strand of the EGFP cDNA. As shown in Fig. 3E, vector genome hybridizations for plus-strand and minus-strand probes were indistinguishable for the various types of viruses (AV2:5/2eGFP, AV2:2/2EGFP, and AV5:5/5eGFP) and demonstrated the anticipated 1:1 ratio for plus and minus strands. Cumulatively, our results demonstrate that hybrid ITR-based vector genomes can efficiently package into viral capsids of AAV-2 or AAV-5 serotypes with an efficiency and fidelity similar to homologous ITR-containing vectors.

To establish that hybrid viruses AV2:5/2eGFP and AV2:5/5eGFP had infectivity similar to homologous ITR-containing vectors AV2:2/2eGFP and AV5:5/5eGFP, we compared the ability of these four vectors to express their encoded EGFP transgene in HeLa cells. After infecting HeLa cells with an equivalent number of DNA-resistant particles (DNase-resistant particles) for each virus, we compared the expression of EGFP for each virus by fluorescence microscopy. The results from this comparison, shown in Fig. 3F, demonstrate indistinguishable levels of EGFP expression between the hybrid ITR viruses (AV2:5/2eGFP and AV2:5/5eGFP) and their homologous ITR counterparts (AV2:2/2eGFP and AV5:5/5eGFP). These results demonstrate that hybrid 2:5 ITR genomes can be packaged with infectious efficiency similar to homologous ITR-containing genomes. The EGFP expression in the group of AAV-5-encapsidated viruses, AV2:5/5eGFP and AV5:5/5eGFP, which was lower than that for AAV-2 capsid vectors, was consistent with the previously reported lower transduction efficiency (~five-fold) of rAAV-5 in HeLa cells (41). In summary, these studies evaluating transgene expression from hybrid ITR vectors demonstrate that ITR homology on either end of the AAV genome is not necessary for functional expression of an encoded transgene.

AV2:5 hybrid ITR viruses less efficiently form circular genomes than AV2:2 or AV5:5 ITR viruses. With the above-characterized hybrid ITR vector, AV2:5/2eGFP, we next sought to test the hypothesis that ITR homology on either end of the AAV genome was needed for efficient formation of viral circular intermediates. If indeed circular intermediates were reduced in AV2:5/2eGFP-infected HeLa cells, compared to

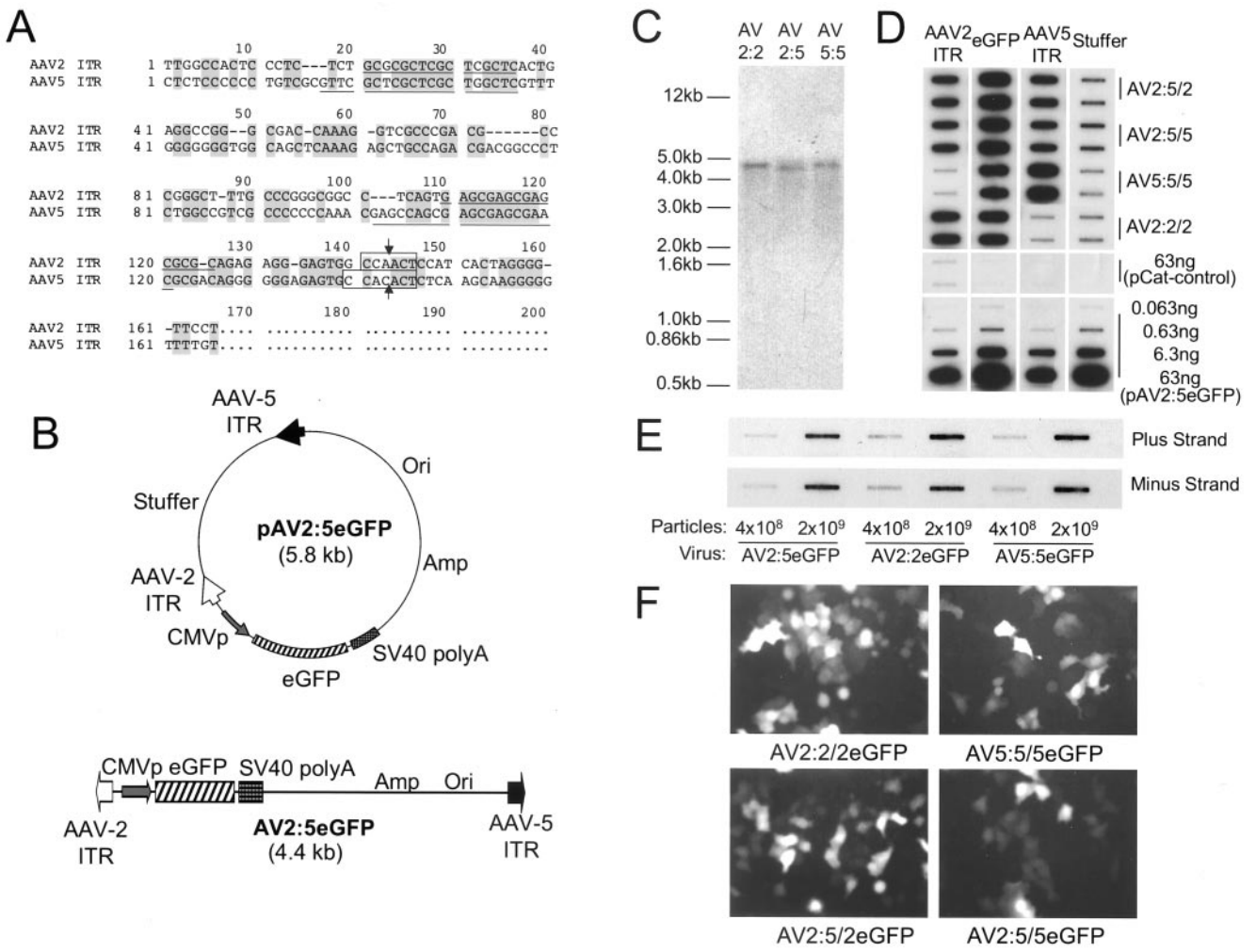

FIG. 3. Hybrid ITR viral genomes produce infectious virus with efficiency similar to that of genomes with homogenous ITR structure. (A) Homology alignment of AAV-2 and AAV-5 ITRs generated by Higgins' arithmetic with DNASIS software. Identical nucleotides in both sequences are indicated by shading. The Rep protein-binding motif is underlined, the terminal resolution site motif (*trs*) is marked with a box, and the site of cleavage in each is indicated with vertical arrows. (B) Schematic structure of the hybrid ITR proviral plasmid pAV2:5eGFP and AV2:5eGFP viral genome. The hybrid ITR vector was packaged into either an AAV-2 or AAV-5 capsid to assemble the AV2:5/2eGFP and AV2:5/5eGFP infectious viruses, respectively. Similar vectors with uniform AAV-2 and AAV-5 ITRs on either end of the genome were used to generate AV2:2/2eGFP and AV5:5/5eGFP viruses, respectively (not diagrammed). (C) Alkaline Southern blot analysis was used to evaluate viral genome integrity from purified AV2:5/2eGFP, AV2:2/2eGFP, and AV5:5eGFP viruses. A uniform band from each vector was visualized with a ^{32}P-labeled EGFP probe in this Southern blot and confirmed the packaging of intact viral genomes for each virus type. (D) Slot blot analysis evaluating DNA from purified viruses with different probes against the AAV-2 ITR, AAV-5 ITR, the EGFP transgene, or stuffer sequences in the backbone of proviral plasmids. pCat is a control plasmid with no sequence homology to any of the probes. pAV2:5eGFP is a control proviral plasmid used to compare hybridization signals for all probes used. Results demonstrate equivalent packaging of both AAV-2 and AAV-5 ITRs in the hybrid vectors and nearly equivalent packaging of stuffer sequences (≈10%) in all vectors. (E) Slot blot analysis was used to evaluate the efficiency of plus- and minus-strand viral genome packaging. Oligonucleotide probes against the sense and antisense strands of EGFP cDNA were used for this analysis. The minus strand of the viral genome was detected with a 44-mer probe, 5′-TCCAGGAGCGCACCATCTTCTTCAAG GACGACGGCAACTACAAG-3′, and the plus viral strand was detected with a complementary probe, 5′-CTTGTAGTTGCCGTCGTCCTT GAAGAAGATGGTGCGCTCCTGGA-3′. Oligonucleotide probes were end labeled with ^{32}P by using T4 polynucleotide kinase and [γ-^{32}P]ATP; 4×10^8 and 2×10^9 DNase-resistant particles of AV2:5/2eGFP, AV2:2/2eGFP, and AV5:5/5eGFP were used for the slot blot hybridization assay. The results demonstrated equivalent ratios of plus- and minus-strand viral genomes for all vectors analyzed. (F) The infectious titer of hybrid ITR viruses (AV2:5/2eGFP and AV2:5/5eGFP) was compared to that achieved with native AV2:2/2eGFP and AV5:5/5eGFP viruses following infection in HeLa cells. HeLa cells were infected with 500 DNase-resistant particles/cell of AV2:2/2eGFP, AV5:5/5eGFP, AV2:5/2eGFP, or AV2:5/5eGFP, and EGFP fluorescent photomicrographs were taken at 48 h postinfection. Hybrid ITR viruses demonstrate levels of transduction similar to that of the native vectors for each serotype. Note that transduction with the AAV-5 capsid virus is approximately four- to fivefold lower than that achieved with AAV-2 capsid vectors in HeLa cells.

AV2:2/2eGFP and AV5:5/2eGFP, this would suggest that ITR homology potentially mediates intramolecular homologous recombination in the formation of monomer circular viral genomes. Similar EGFP expression was seen 2 days postinfection in the HeLa cells transduced with these three AAV-2 capsid-packaged viruses (data not shown); however, the number of ampicillin-resistant colonies that were rescued from the Hirt DNA extracted from the AV2:5/2eGFP-infected cells was sig-

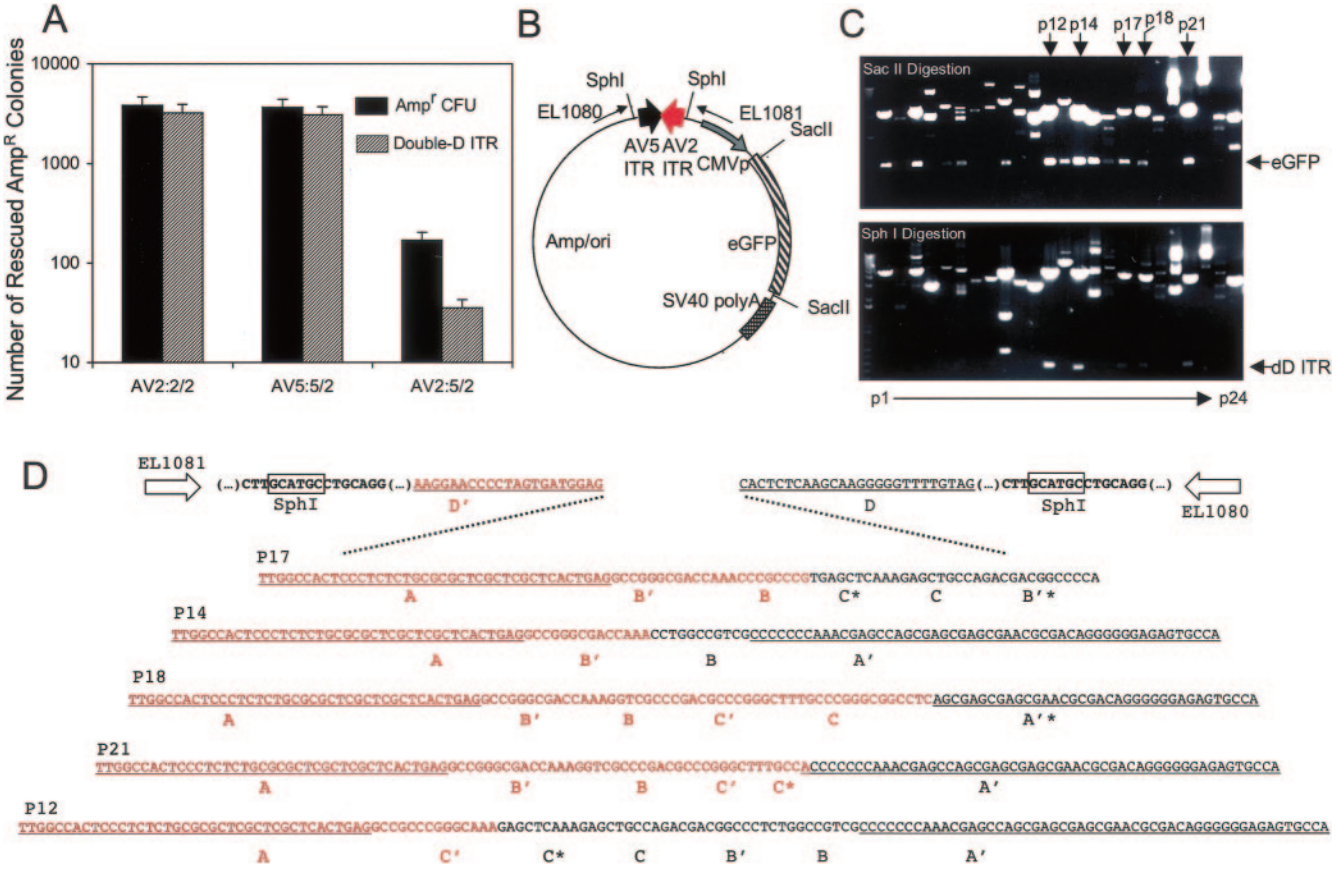

FIG. 4. Hybrid AV2:5 ITR viral genomes have reduced capacity to form circular intermediates. HeLa cells were infected at a multiplicity of infection of 500 DNase-resistant particles/cell with AV2:2/2eGFP, AV5:5/2eGFP, or AV2:5/2eGFP virus. The low-molecular-weight Hirt DNA was extracted at 1 day postinfection, and 1/10th of the DNA was used to transform *E. coli* Sure cells. (A) Total rescued ampicillin-resistant CFU and head-to-tail circular intermediates with double-D ITR junctions are indicated. Results indicate the mean (± standard error of the mean) for triplicate assays for each experimental point. (B) The predicted structure of a head-to-tail circularized hybrid ITR genome is given with restriction enzyme sites and sequence primers used for molecular characterization. (C) Restriction enzyme analysis of 24 circular intermediates rescued following AV2:5/2eGFP infection. Isolated plasmids p12, p14, p17, p18, and p21 (marked by arrows) were the only five clones that demonstrated an intact 800-bp EGFP SacII fragment and a ≈200-bp ITR SphI fragment that matched the predicted double-D circular intermediate structure seen with the AV2:2 and AV5:5 genomes. These clones were further analyzed by sequencing of the ITR junction with primers EL1080 and EL1081. (D) Sequence results of the five clones containing a double-D ITR junction. The upper line depicts consistent sequences found in all clones and includes an intact D′ sequence from the AAV-5 and AAV-2 ITRs. The boldface partial sequence is the area flanking the ITRs where the SphI site (boxed) resides. Below is the remaining sequence between the two D sequences for each of the individual clones, as marked. The sequence homology to AAV-5 ITR is indicated in black, and homology to AAV-2 ITR is indicated in red. The various palindromic segments of the ITR are indicated by D, A′ B, B′, C, C′, and A, according to the standard nomenclature. The D′ and A segments of the AAV-2 ITR and the A′ and D segments of AAV-5 are marked with underlining. Segments with deletions are marked by an asterisk.

nificantly lower (22-fold) than that for AV2:2/2eGFP and AV5:5/2eGFP viruses with homologous ITRs (Fig. 4A).

We randomly selected 24 plasmids rescued from AV2:5/2eGFP-infected cells for structural analysis. Molecular characterization of these rescued plasmids was performed by slot blot hybridization assays with ^{32}P-labeled probes against the cytomegalovirus promoter, EGFP cDNA, AAV-2 ITR, and AAV-5 ITR; restriction enzyme analyses; and sequencing of the predicted double-D ITR junction. The hybridization results of the 24 rescued plasmids demonstrated that 16 were positive for both the cytomegalovirus promoter and EGFP probes, of which six were also positive for both AAV-2 and AAV-5 ITRs. The remaining eight colonies (33%) were positive for either AAV-2 or AAV-5 ITRs only (data not shown). The percentage of rescued plasmids that were positive for all probes spanning the viral genome was significantly lower for the AV2:5 hybrid vector (25%) than for homologous AV2:2 or AV5:5 vectors (≈94%).

Restriction enzyme analyses were also performed to better define the heterogeneity in the structure of these 24 plasmid clones (Figs. 4B and C). Figure 4B depicts the predicted structure of circular monomer hybrid AV2:5eGFP genome in a head-to-tail conformation. SacII digestion of such an intermediate would release a ≈800-bp EGFP fragment, while SphI digestion would be expected to release a ≈200-bp AAV-2 and AAV-5 double-D ITR junction. As expected from the hybridization studies, restriction enzyme analyses demonstrated a considerably higher level of variability in the structure of the rescued clones derived from AV2:5/2eGFP-infected cells than from AV2:2/2eGFP- or AV5:5/2eGFP-infected cells. Only 13

of the 16 EGFP-hybridizing clones retained an intact 800-bp SacII fragment. An even lower percentage of clones (5 out of 24) gave rise to a ≈200-bp SphI fragment, predicted to be a double-D AAV2-AAV5 ITR junction.

Sequence analysis of the ITR junction in these clones (Fig. 4D) demonstrated considerable variability in the recombination site between the AV2 and AV5 ITRs as well as variable internal deletions. When similar restriction enzyme analysis was used to screen for double-D ITR junctions in rescued plasmids from AV2:2/2eGFP- and AV5:5/2eGFP-infected cells, 93.4% and 89.7% of the clones tested released a small fragment representing the double-D ITR junction, respectively (data not shown). When considering the total number of Amp^r colonies rescued from Hirt DNA and the percentage of rescued plasmids that contained a double-D ITR array, these data demonstrate that the frequency at which AV2:5/2eGFP viruses generated double-D circular intermediates was ≈100-fold lower than that for viruses with homologous ITRs on either end of the genome (Fig. 4A). These results strongly suggest that ITR sequence homology on either end of the viral genomes likely plays a key role in the circularization of the AAV genome.

One limitation of the above analysis is worth noting. Circular head-to-head and tail-to-tail dimers and concatemers are not replication competent in bacteria due to opposing origins of replication. Therefore, such intermediates cannot be rescued in the bacteria without significant deletion during the bacterial rescue process. However, we have previously demonstrated that head-to-head and tail-to-tail dimers can form through intermolecular recombination with a two-vector system (only one of which contains an *ori* and ampicillin resistance gene) (43, 44). Hence, although we could conclude that hybrid ITR vectors do not efficiently form double-D circular monomers, we could not determine the extent to which intermolecular recombination might occur in the formation of circular head-to-head and tail-to-tail dimers.

To gain further insight into the molecular differences of genome conversion between hybrid and homologous ITR vectors, we analyzed the molecular forms of AAV genomes in Hirt DNA from AV2:2/2eGFP- and AV2:5/2eGFP-infected cells. The goal of this assay was to directly distinguish between the abundance of linear and circular monomers or dimer molecules by Southern blotting. In this assay we chose StuI as a diagnostic restriction site to distinguish between the various molecular forms. StuI cuts once at the end of the cytomegalovirus promoter and would only digest double-stranded viral genomes. As shown in Fig. 5A, StuI digestion followed by Southern blotting with a cytomegalovirus probe produced a 940-bp fragment from linear monomer and head-to-tail and tail-to-tail dimer viral genomes. Head-to-tail linear dimer genomes and head-to-tail circular genomes also produced a 4.7- or 4.4-kb linear fragment, depending on the vector type. In contrast, head-to-head linear and head-to-head/tail-to-tail circular dimers produced a unique 1.88-kb fragment for both vector types.

The results of Southern blot analysis (Fig. 5B) for AV2:2eGFP demonstrated that StuI digestion produced cytomegalovirus-hybridizing bands of 940 bp and 4.7 kb, which is consistent with linear and circular head-to-tail intermediates, respectively. Furthermore, undigested DNA samples gave rise to previously described supercoiled monomer circular intermediates (8, 31) that migrated at 2.8 kb and shifted in size to linear 4.7-kb fragments following digestion with StuI. Single-stranded viral genomes, which remain as the predominant form at 2 days postinfection, were unchanged by StuI digestion. In stark contrast to AV2:2eGFP, AV2:5eGFP Hirt DNA demonstrated a significantly increased abundance of the StuI 940-bp end fragment and a lack of circular viral genomes in the undigested sample. Notably, a large percentage of AV2:5eGFP viral genomes migrated as a smear between 1 and 1.4 kb in the undigested Hirt DNA, a finding not observed with the AV2:2eGFP sample.

Despite the fact that the majority of these AV2:5 heterogeneous genomes had a clear double-stranded end fragment (as suggested by StuI digestion), their exact structure(s) remains unclear. These genomes appear to have a highly variable secondary structure and may have partially synthesized second strands. Although linear, double-stranded genomes certainly existed in AV2:2-infected cells (as indicated by the 940-bp cytomegalovirus-hybridizing end fragment following StuI digestion), their abundance was significantly reduced in comparison to that of AV2:5eGFP-infected cells. These findings are most consistent with increased abundance of linear monomer genomes with hybrid ITR vectors. Such differences between the abundance of linear and circular genomes for AV2:2eGFP and AV2:5eGFP vectors are also consistent with the Hirt DNA bacterial rescue experiment.

One additional difference observed between homologous (AV2:2eGFP) and hybrid (AV2:5eGFP) ITR vectors at 2 days postinfection (Fig. 5B) was the apparent greater stability of the hybrid ITR genomes. To confirm this finding, Hirt DNAs were extracted from AV2:2eGFP- and AV2:5eGFP-infected HeLa cells at different time points and visualized by Southern blotting, as shown in Fig. 5C. Comparing the internalized AV2:2eGFP and AV2:5eGFP genomes at an early time point of 6 h postinfection demonstrated no significant differences in the amount of DNA endocytosed by HeLa cells for both viruses. However, the level of detectable AV2:2eGFP genomes was significantly reduced after 2 days postinfection and became barely detectable by 5 days postinfection. Although we noticed a similar trend of time-dependent disappearance of hybrid ITR viral genome, the rate of diminishing viral genome signal was obviously slower than that for AV2:2eGFP. A significantly greater fraction of AV2:5eGFP viral genomes remained at 5 days postinfection in comparison to AV2:2eGFP-infected cells. We interpret the lack of distinctly visible genome intermediates (i.e., linear or circular concatemers) in AV2:2eGFP-infected cells at later time points to reflect more heterogeneity in the apparent migration position size due to differences in supercoiling of homologous ITR vector genome concatemers.

This notion is supported by the diverse sizes of circular concatemers rescued from rAAV-2-infected mouse muscle at long times postinfection (8, 44). Alternatively, altered rates of dilution of viral DNA following cell division might also account for these observations. Since gene expression from these two types of vectors was nearly equivalent and did not change over time (data not shown), it appears that a smaller fraction of hybrid ITR genomes remaining at 5 days posttransfection are capable of expressing transgenes in comparison to homologous ITR vector genomes. Indeed, the migration pattern of hybrid

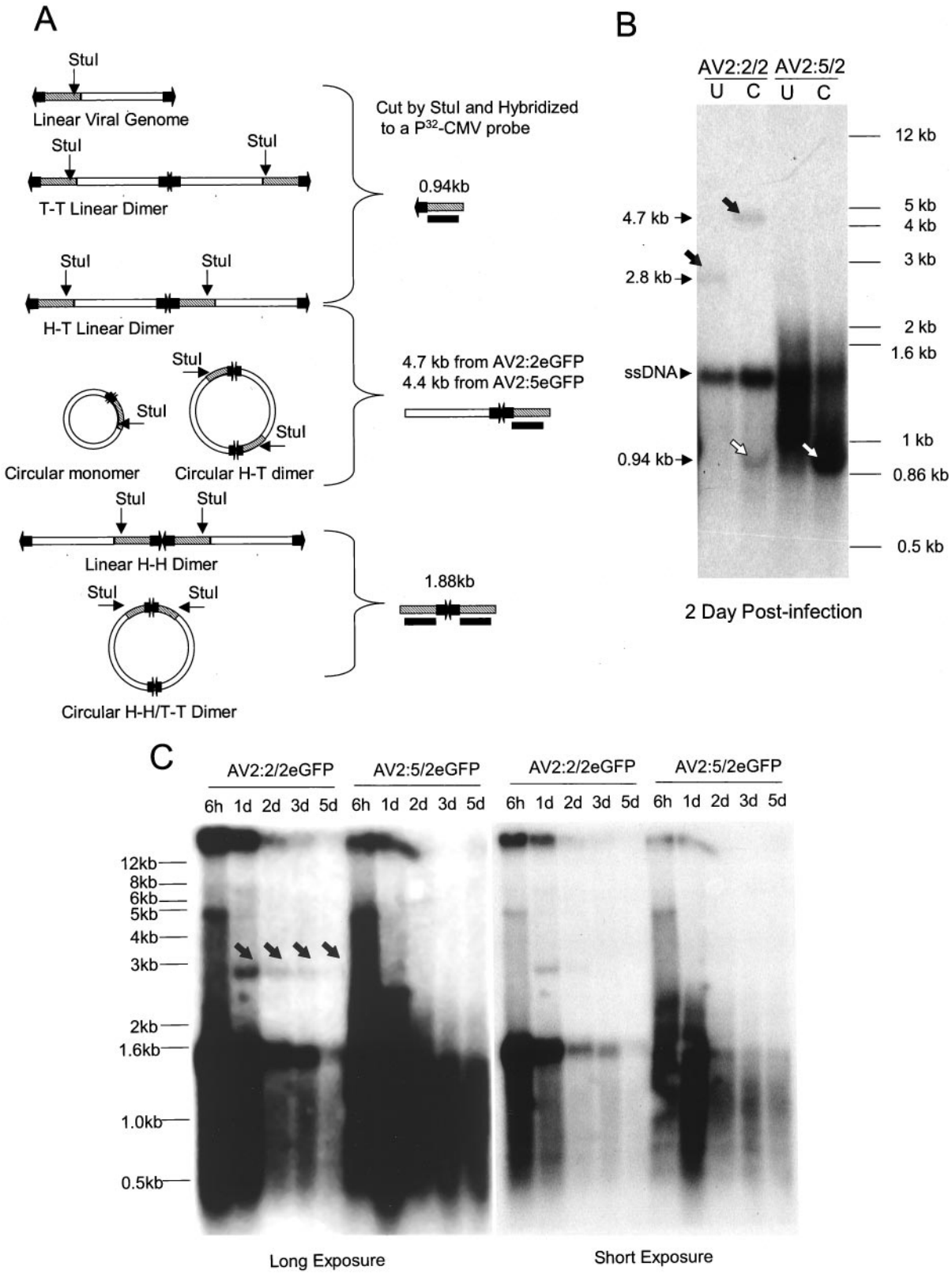

FIG. 5. Southern blot analysis of Hirt DNA extracted from AV2:5/2eGFP- and AV2:2/2eGFP-infected HeLa cells. HeLa cells were infected with AV2:2/2eGFP and AV2:5/2eGFP at a multiplicity of infection of 500 DNase-resistant particles/cell, and Hirt DNAs were extracted at different time points postinfection. One-quarter of the Hirt DNA from each sample was resolved on a 1.2% agarose gel, and Southern blotting of viral DNA was performed with a ^{32}P-labeled probe against the cytomegalovirus promoter. (A) Schematic representation of the predicted StuI digestion products from possible double-stranded transduction intermediates. H-H, head-to-head; T-T, tail-to-tail; H-T, head-to-tail. (B) Hirt DNA samples

ITR genomes at 5 days postinfection remained very heterogeneous and may reflect different secondary structures with altered capacities to express an encoded transgene. These predominantly linear hybrid ITR vector genomes, although less transcriptionally active, appear to have increased stability over homologous ITR vector genome conversion products.

Hybrid AV2:5 ITR genomes facilitate directional intermolecular recombination and enhance the efficiency of dual-vector trans-splicing approaches. The results from Hirt DNA Southern blot analysis and bacterial rescue experiments have suggested that the ITR homology on either end of the rAAV genome plays a key role in rAAV genome circularization. These findings provide direct evidence that intramolecular circularization of AAV genomes is an ITR sequence-dependent recombination process. The generation of hybrid vectors with reduced capacity to form monomer circular intermediates also afforded the opportunity to address the involvement of these structures as precursors to intermolecular heterodimers. The formation of intermolecular heterodimers is the foundation of dual-vector technologies capable of increasing the functional capacity of rAAV to deliver large transgenes that cannot be packaged into a single-vector genome. To this end, we sought to use hybrid ITR vectors to investigate the underlying mechanisms responsible for generating heterodimers as a basis for potentially improving the efficiency of dual-vector approaches for gene therapy.

A dual-vector trans-splicing approach was used to functionally assess the extent of intermolecular recombination by reconstituting a *lacZ* transgene product from two *lacZ* minigene exons independently delivered by two vectors. In this context, reconstitution of β-galactosidase is a direct measure of directional head-to-tail intermolecular recombination events between two independent viral genomes. To this end, we constructed a dual-vector set based on hybrid ITR vector genomes (AV5:2LacZdonor and AV2:5LacZacceptor), as shown in Fig. 6A, and compared their ability for intermolecular recombination with that of a homologous ITR vector set (AV2:2LacZ donor and AV2:2LacZacceptor). Both donor and acceptor viral genomes were packaged into AAV-2 and AAV-5 capsid virions for analysis in HeLa cells. The infectious titer of all eight viruses was compared individually by infecting HeLa cells with equivalent physical titers (2.5×10^3 DNase-resistant particles/cell) and assessing DNA uptake into cells at 16 h postinfection. This method was used because an appropriate cell line was unavailable for mobilization assays for hybrid vectors (i.e., requiring both type 2 and 5 Rep proteins). These studies confirmed that all eight viral stocks (AV2:2LacZdonor, AV2:2LacZacceptor, AV5:2LacZdonor, and AV2:5lacZdonor in AAV-2 and AAV-5 capsids) delivered similar levels of viral DNA into cells for each of the capsid serotypes (data not shown). These data support functional analyses demonstrating similar abilities of hybrid and homologous ITR vectors to express a GFP-encoded transgene in HeLa cells (Fig. 3F).

Functional studies evaluating the ability for intermolecular concatemerization were similarly performed in HeLa cells coinfected with donor and acceptor vectors for each serotype and ITR configuration (Fig. 6B and C). Relative β-galactosidase activities for each vector set were assayed at 3 days postinfection. The results from these experiments demonstrated that hybrid ITR dual-vector sets were sixfold (Fig. 6B) or 10-fold (Fig. 6C) more effective at reconstituting a functional *lacZ* gene product than homologous ITR vectors with AAV-2 or AAV-5 capsids, respectively. Given the findings that hybrid ITR vectors preferentially increase the abundance of linear-form genomes (Fig. 5B), these findings suggest that concatemerization of AAV linear genomes occurs in a sequence-specific fashion through ITR homologous recombination. In this context, the sequence homology of the two types of ITRs in hybrid vectors would be expected to preferentially drive the formation of functional heterodimers.

To provide further evidence for sequence-restricted ITR recombination in the formation of heterodimers, we also compared the efficiency of trans-splicing between various combinations of homologous ITR and hybrid ITR vector sets. As expected, the results from these experiments demonstrated that the AV5:2/2LacZdonor and AV2:2/2LacZacceptor or AV2:2/2LacZdonor and AV2:5/2LacZacceptor vector combination gave an intermediate level of transgene reconstitution to homologous and hybrid vector sets (Fig. 6D). These results provide further evidence for the importance of ITR sequences in heterodimer formation.

DISCUSSION

Because circularization of rAAV genomes has only been studied in the context of AAV-2 ITR-containing genomes, we felt that a clearer understanding of this process for other divergent AAV serotypes would help clarify the overall importance of circular genomes in rAAV transduction. To this end, we first evaluated circular intermediate formation from AAV-5 ITR-containing vectors because they are the least conserved in primary sequence to AAV-2. With an AV5:5/5eGFP shuttle vector, we discovered that 94% of rescued circular intermediates had a head-to-tail double-D ITR structure similar to that observed with the AV2:2/2eGFP vector. Although differences in the abundance of double-D ITR circular intermediates were observed with these cap5- and cap2-based vectors, due to differences in tropism for transducing HeLa cells, subsequent analysis comparing the AV2:2/2eGFP and AV5:5/2eGFP viruses demonstrated an indistinguishable abundance of circular double-D ITR genomes following infection. These results conclusively demonstrate that AAV-5-based vectors have efficien-

at 2 days postinfection were digested with StuI and analyzed by Southern blotting with a cytomegalovirus probe. The open arrows point to a 0.94-kb band end fragment diagnostic for the existence of linear viral genomes. Solid arrows point to bands diagnostic for monomer supercoiled circular intermediates in the uncut sample (2.8 kb) and linear full-length genomes in the StuI-digested sample (4.7 kb). The migration of single-stranded viral DNA (ssDNA) is also marked. U, undigested; C, StuI digested. (C) Undigested Hirt DNAs extracted from AV2:2/2eGFP- and AV2:5/2eGFP-infected HeLa cells at 6 h, 1 day, 2 days, 3 days, and 5 days postinfection were analyzed by Southern blotting. Solid arrows point to a 2.8-kb band previously characterized as supercoiled circular monomers (32), which is visible only AV2:2/2eGFP-infected cells.

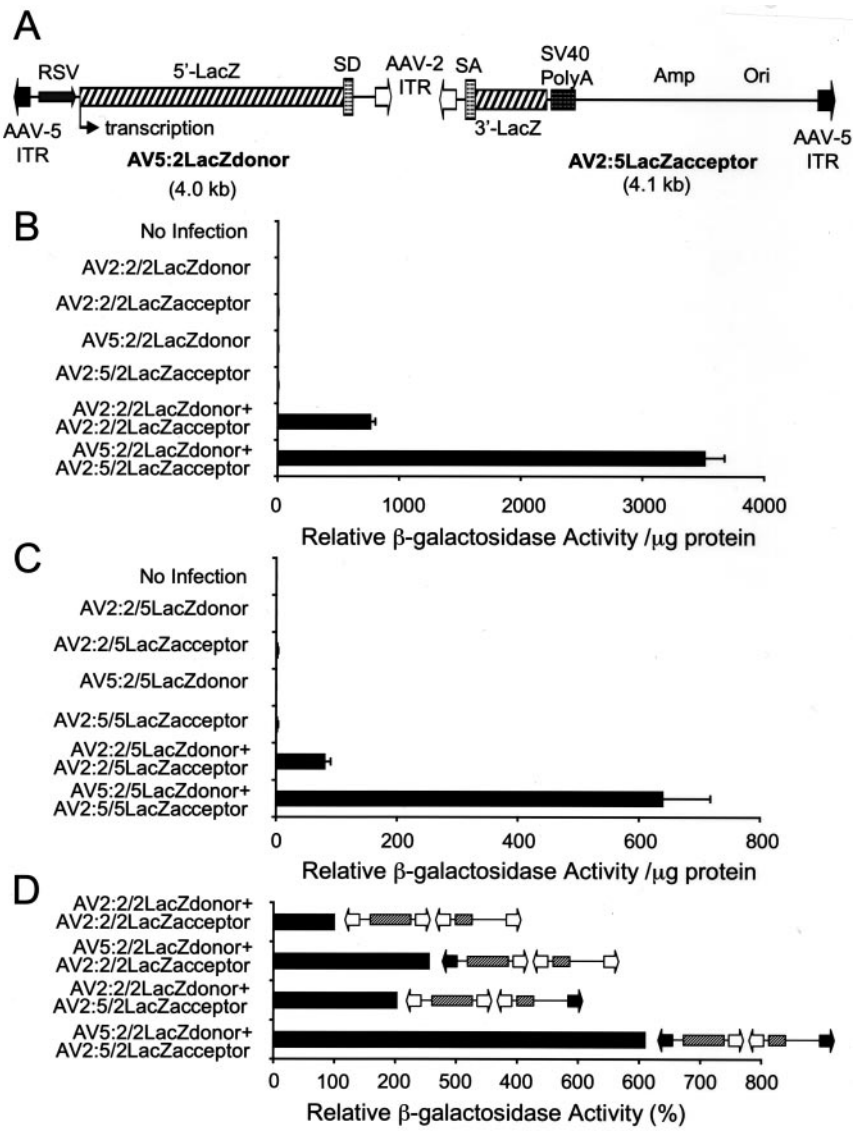

FIG. 6. Comparison of dual-vector heterodimerization between hybrid and homologous ITR vectors. Dual-vector reconstitution of a *lacZ* minigene was used to evaluate the extent of tail-to-head intermolecular recombination with hybrid and homologous ITR vectors. (A) Schematic representation of the hybrid ITR trans-splicing viral genomes, AV5:2LacZdonor and AV2:5LacZacceptor, which were used to generate AAV-2 serotype viruses AV5:2/2LacZdonor and AV2:5/2LacZacceptor, respectively. The AV2:2/2LacZdonor and AV2:2/2LacZacceptor viruses (not shown) had similar structures but contained AAV-2 ITRs on both ends of the genome. (B to D) HeLa cells were infected at a multiplicity of infection of 2,500 DNase-resistant particles/cell with each virus alone or in combination, as indicated. β-Galactosidase activity was quantified at 3 days postinfection. This analysis was performed with (B) AAV-2-encapsidated viruses and (C) AAV-5-encapsidated viruses. (D) Mixing experiments with combinations of hybrid and homologous ITR donor and acceptor vectors were also performed to assess sequence specificity in ITR recombination. Vector combinations are shown schematically on the graph, with open and solid arrowheads indicating AAV-2 and AAV-5 ITRs, respectively. Data represent the mean (± standard error of the mean) of seven independent infections.

cies of circular intermediate formation similar to those of AAV-2 genomes despite altered sequence homology of the ITRs. They also suggest that circularization is likely a common pathway for all serotypes of rAAV.

Consequently, we sought to more clearly understand the role of ITRs in circular intermediate formation and the subsequent concatemerization processes of rAAV genomes. To this end, we generated a novel AAV2:5 hybrid ITR virus to address the involvement of AAV ITRs in the process of viral genome circularization and concatemerization. Studies evaluating hybrid ITR vectors (AV2:5/2eGFP and AV2:5/5eGFP) demonstrated that they were as functional as homologous ITR-containing vectors (AV2:2/2eGFP and AV5:5/5eGFP) in expressing an encoded EGFP transgene. These findings demonstrate that homologous ITRs on both ends of the viral genome are not necessary for efficient second-strand synthesis. Interestingly, the AV2:5/2eGFP virus had a substantially lower ability to form circular intermediates than the AV2:2/2eGFP and AV5:5/2eGFP viruses. Furthermore, the circular intermediates that were recovered from the hybrid ITR virus were

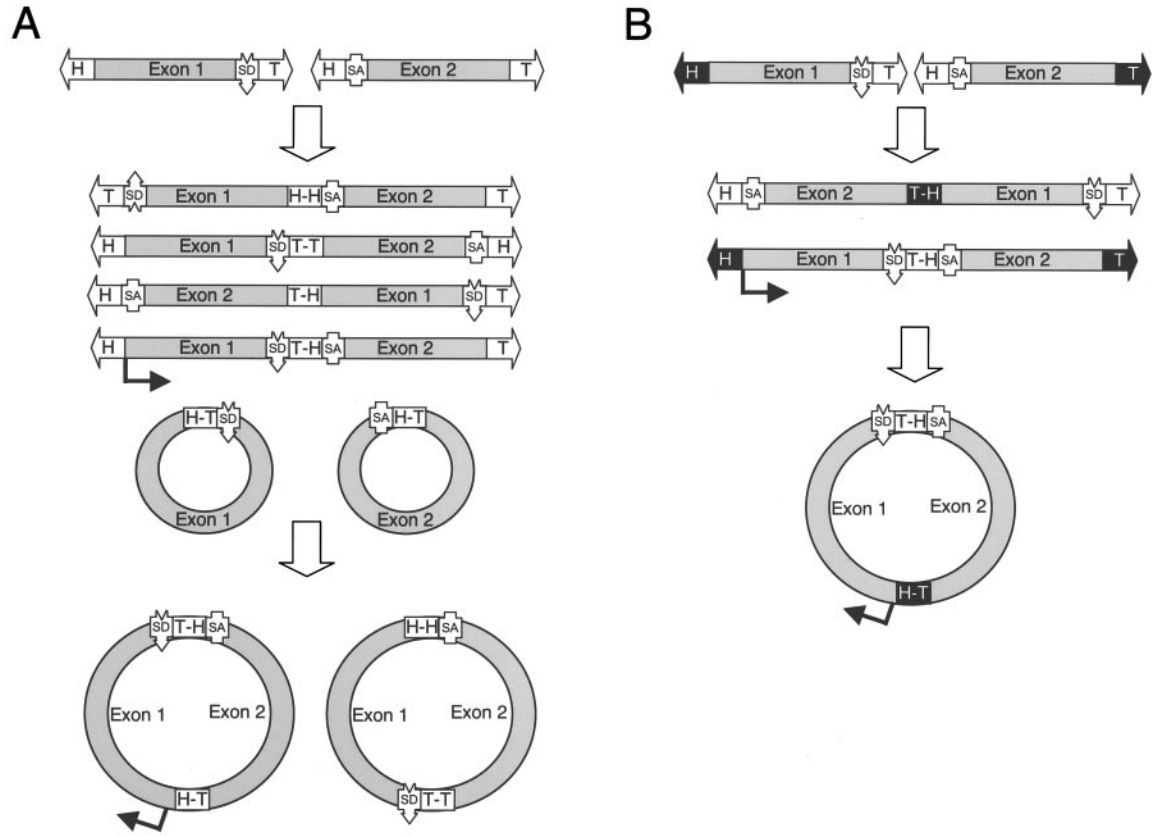

FIG. 7. Hybrid ITR vectors facilitate directional heterodimerization more efficiently than homologous ITR vectors. Hybrid ITR vectors have been shown to more efficiently reconstitute dual-vector trans-spliced transgenes than homologous ITR vectors. Based on molecular analysis of circular and linear intermediates from these two vector types, working hypotheses regarding intermolecular and intramolecular recombination events can be derived for (A) homologous ITR vectors and (B) hybrid ITR vectors. (A) Predicted transduction intermediates and possible intermolecular heterodimers are shown for homologous ITR vectors. With this vector type, 25% of linear dimers are capable of reconstituting a dually encoded minigene (marked by an arrow). Circular dimers are derived either from recombination between circular monomers or by circularization of linear dimers; 50% of circular dimers generated by either of these two processes would be expected to reconstitute a functional minigene. (B) In contrast, hybrid ITR vectors inefficiently form circular monomers, and 50% of linear heterodimers would be expected to reconstitute a functional minigene. However, self-circularization of these two forms of linear heterodimers is also expected to occur via ITR-mediated homologous recombination. If such events occur, all the resulting circular heterodimers will be competent to functionally trans-splice, and the probability of reconstituting the functional minigene will be even higher. This working model helps to explain how hybrid ITR vectors may be capable of greatly enhancing dual-vector trans-splicing approaches by altering the equilibrium of various viral genome intermediates within the cell.

much more heterogeneous in structure and maintained deletion of both the ITRs and EGFP transgene. The abundance of double-D ITR-intact circular genomes (containing EGFP and ITRs) was 100-fold less for AV2:5/2eGFP than for the AV2:2/2eGFP and AV5:5/2eGFP viruses. These findings suggest that ITR-mediated homology at both ends of the viral genome is important for directing intramolecular circularization of the rAAV genome. However, this circularization process is not necessary for expression of encoded gene products. Hence, both the double-stranded linear and circular transduction intermediates are competent for transgene expression.

Although our studies with EGFP-encoding hybrid ITR vectors provided evidence for the importance of ITR sequences in self-circularization, similar requirements for the ITR in intermolecular recombination of viral genomes could not be directly assessed in these studies. Several precursor viral genome forms could conceivably be involved in the formation of intermolecular heterodimers and concatemers, including single-stranded linear, double-stranded linear, single-stranded circular, and double-stranded circular genomes. Recently, studies evaluating sequentially infected mouse tibialis muscles with *lacZ* trans-splicing vectors have suggested that recombination between double-stranded viral genomes is the predominant pathway for concatemerization (10). These studies also suggested that the majority of internalized rAAV genomes remained as single-stranded DNA, while only a small fraction were converted to the functional, double-stranded transduction intermediates responsible for circularization and concatemerization.

In muscle, circular monomer intermediates have been thought to play an important role as precursors to intermolecular recombination at double-D ITRs (8, 9). However, evidence supporting this hypothesis has been indirect and predominantly based on the types of intermolecular concatemers that are formed over time. In this context, both tail-to-head and head-to-head/tail-to-tail intermolecular circular concate-

mers could be rescued from muscle Hirt DNA following coinfection with two independent vectors (43, 44). These findings support the hypothesis that the process of recombination between circular intermediates is bidirectional and facilitated by double-D ITRs. Although these studies demonstrate the existence of circular concatemers with various genome orientations, they were not directly capable of evaluating the extent to which functional linear heterodimers were formed.

Our findings in the present study demonstrating that hybrid ITR vectors have a ≈100-fold reduced capacity to form double-D circular genomes provided the opportunity to directly evaluate the involvement of these structures in heterodimer formation with functional gene expression assays. Contrary to our original hypothesis, hybrid ITR vectors demonstrated increased directional heterodimer formation. This observation, together with the findings from homologous and hybrid ITR vector-mixing experiments, support the involvement of sequence-specific ITR recombination of linear viral genomes. These findings are in stark contrast to previous data by others suggesting that ITR sequences do not enhance concatemerization of synthetic linear AAV genomes in the liver (25). The reason for the discrepancy between these earlier findings in the liver and our present studies is currently unknown but could involve cell type-specific differences or differences in the model systems used to evaluate concatemerization.

Given the documented involvement of circular concatemers as AAV genome intermediates, we believe our study favors an interpretation that both linear and circular genomes can participate in concatemerization processes (Fig. 7). In the context of hybrid ITR vectors, the equilibrium appears to have shifted to favor linear concatemerization. These findings are reminiscent of findings in SCID mice, for which increased linear concatemers were formed in the absence of DNA-Pkcs (34). However, unlike previous analyses in the muscles of SCID mice, which did not demonstrate increased dual-vector trans-splicing (10), our studies with hybrid ITR vectors favored a directional linear intermolecular recombination event (Fig. 7).

Unlike homologous ITR vectors, in which recombination between ITRs leads to random orientation of genome concatemers, hybrid ITR vectors can now allow directionally dependent concatemerization, which increases the number of functional genomes obtained with dual-vector trans-splicing approaches. Furthermore, the ability to alter concatemerization and the ratio of circular to linear genomes by altering ITR sequences may prove useful for modulating other aspects of rAAV-mediated gene therapy, such as the extent of integration and the stability of expression.

ACKNOWLEDGMENTS

This work was supported by NIH RO1 HL58340 (J.F.E.), the Targeted Genetics Corporation, and the Gene Therapy Center (DK54759).

We thank Leah Williams and Greg Leno for editorial assistance with the manuscript.

REFERENCES

1. **Berns, K. I., and C. Giraud.** 1996. Adeno-associated virus (AAV) vectors in gene therapy. Springer, New York, N.Y.
2. **Carter, P. J., and R. J. Samulski.** 2000. Adeno-associated viral vectors as gene delivery vehicles. Int. J. Mol. Med. **6:**17–27.
3. **Chao, H., Y. Liu, J. Rabinowitz, C. Li, R. J. Samulski, and C. E. Walsh.** 2000. Several log increase in therapeutic transgene delivery by distinct adeno-associated viral serotype vectors. Mol. Ther. **2:**619–623.
4. **Chiorini, J. A., S. Afione, and R. M. Kotin.** 1999. Adeno-associated virus (AAV) type 5 Rep protein cleaves a unique terminal resolution site compared with other AAV serotypes. J. Virol. **73:**4293–4298.
5. **Chiorini, J. A., F. Kim, L. Yang, and R. M. Kotin.** 1999. Cloning and characterization of adeno-associated virus type 5. J. Virol. **73:**1309–1319.
6. **Douar, A. M., K. Poulard, D. Stockholm, and O. Danos.** 2001. Intracellular trafficking of adeno-associated virus vectors: routing to the late endosomal compartment and proteasome degradation. J. Virol. **75:**1824–1833.
7. **Duan, D., P. Sharma, L. Dudus, Y. Zhang, S. Sanlioglu, Z. Yan, Y. Yue, Y. Ye, R. Lester, J. Yang, K. J. Fisher, and J. F. Engelhardt.** 1999. Formation of adeno-associated virus circular genomes is differentially regulated by adenovirus E4 ORF6 and E2a gene expression. J. Virol. **73:**161–169.
8. **Duan, D., P. Sharma, J. Yang, Y. Yue, L. Dudus, Y. Zhang, K. J. Fisher, and J. F. Engelhardt.** 1998. Circular intermediates of recombinant adeno-associated virus have defined structural characteristics responsible for long term episomal persistence in muscle. J. Virol. **72:**8568–8577.
9. **Duan, D., Z. Yan, Y. Yue, and J. F. Engelhardt.** 1999. Structural analysis of adeno-associated virus transduction intermediates. Virology **261:**8–14.
10. **Duan, D., Y. Yue, and J. F. Engelhardt.** 2003. Consequences of DNA-dependent protein kinase catalytic subunit deficiency on recombinant adeno-associated virus genome circularization and heterodimerization in muscle tissue. J. Virol. **77:**4751–4759.
11. **Duan, D., Y. Yue, and J. F. Engelhardt.** 2001. Expanding AAV packaging capacity with trans-splicing or overlapping vectors: a quantitative comparison. Mol. Ther. **4:**383–391.
12. **Duan, D., Y. Yue, Z. Yan, and J. F. Engelhardt.** 2000. A new dual-vector approach to enhance recombinant adeno-associated virus-mediated gene expression through intermolecular cis activation. Nat. Med. **6:**595–598.
13. **Duan, D., Y. Yue, Z. Yan, J. Yang, and J. F. Engelhardt.** 2000. Endosomal processing limits gene transfer to polarized airway epithelia by adeno-associated virus. J. Clin. Investig. **105:**1573–1587.
14. **Flotte, T., B. Carter, C. Conrad, W. Guggino, T. Reynolds, B. Rosenstein, G. Taylor, S. Walden, and R. Wetzel.** 1996. A phase I study of an adeno-associated virus-CFTR gene vector in adult CF patients with mild lung disease. Hum. Gene Ther. **7:**1145–1159.
15. **Fu, H., J. Muenzer, R. J. Samulski, G. Breese, J. Sifford, X. Zeng, and D. M. McCarty.** 2003. Self-complementary adeno-associated virus serotype 2 vector: global distribution and broad dispersion of AAV-mediated transgene expression in mouse brain. Mol. Ther. **8:**911–917.
16. **Girod, A., M. Ried, C. Wobus, H. Lahm, K. Leike, J. Kleinschmidt, G. Deleage, and M. Hallek.** 1999. Genetic capsid modifications allow efficient re-targeting of adeno-associated virus type 2. Nat. Med. **5:**1052–1056.
17. **Grimm, D., and M. A. Kay.** 2003. From virus evolution to vector revolution: use of naturally occurring serotypes of adeno-associated virus (AAV) as novel vectors for human gene therapy. Curr. Gene Ther. **3:**281–304.
18. **Hagstrom, J. N., L. B. Couto, C. Scallan, M. Burton, M. L. McCleland, P. A. Fields, V. R. Arruda, R. W. Herzog, and K. A. High.** 2000. Improved muscle-derived expression of human coagulation factor IX from a skeletal actin/CMV hybrid enhancer/promoter. Blood **95:**2536–2542.
19. **Kay, M. A., C. S. Manno, M. V. Ragni, P. J. Larson, L. B. Couto, A. McClelland, B. Glader, A. J. Chew, S. J. Tai, R. W. Herzog, V. Arruda, F. Johnson, C. Scallan, E. Skarsgard, A. W. Flake, and K. A. High.** 2000. Evidence for gene transfer and expression of factor IX in haemophilia B patients treated with an AAV vector. Nat. Genet. **24:**257–261.
20. **McCarty, D. M., H. Fu, P. E. Monahan, C. E. Toulson, P. Naik, and R. J. Samulski.** 2003. Adeno-associated virus terminal repeat (TR) mutant generates self-complementary vectors to overcome the rate-limiting step to transduction in vivo. Gene Ther. **10:**2112–2118.
21. **McCarty, D. M., P. E. Monahan, and R. J. Samulski.** 2001. Self-complementary recombinant adeno-associated virus (scAAV) vectors promote efficient transduction independently of DNA synthesis. Gene Ther. **8:**1248–1254.
22. **Miller, D. G., E. A. Rutledge, and D. W. Russell.** 2002. Chromosomal effects of adeno-associated virus vector integration. Nat. Genet. **30:**147–148.
23. **Musatov, S. A., T. A. Scully, L. Dudus, and K. J. Fisher.** 2000. Induction of circular episomes during rescue and replication of adeno-associated virus in experimental models of virus latency. Virology **275:**411–432.
24. **Nakai, H., S. Fuess, T. A. Storm, L. A. Meuse, and M. A. Kay.** 2003. Free DNA ends are essential for concatemerization of synthetic double-stranded adeno-associated virus vector genomes transfected into mouse hepatocytes in vivo. Mol. Ther. **7:**112–121.
25. **Nakai, H., E. Montini, S. Fuess, T. A. Storm, L. Meuse, M. Finegold, M. Grompe, and M. A. Kay.** 2003. Helper-independent and AAV-ITR-independent chromosomal integration of double-stranded linear DNA vectors in mice. Mol. Ther. **7:**101–111.
26. **Nakai, H., T. A. Storm, and M. A. Kay.** 2000. Increasing the size of rAAV-mediated expression cassettes in vivo by intermolecular joining of two complementary vectors. Nat. Biotechnol. **18:**527–532.
27. **Nakai, H., T. A. Storm, and M. A. Kay.** 2000. Recruitment of single-stranded recombinant adeno-associated virus vector genomes and intermolecular recombination are responsible for stable transduction of liver in vivo. J. Virol. **74:**9451–9463.

28. **Nony, P., G. Chadeuf, J. Tessier, P. Moullier, and A. Salvetti.** 2003. Evidence for packaging of rep-cap sequences into adeno-associated virus (AAV) type 2 capsids in the absence of inverted terminal repeats: a model for generation of rep-positive AAV particles. J. Virol. **77:**776–781.
29. **Reich, S. J., A. Auricchio, M. Hildinger, E. Glover, A. M. Maguire, J. M. Wilson, and J. Bennett.** 2003. Efficient trans-splicing in the retina expands the utility of adeno-associated virus as a vector for gene therapy. Hum. Gene Ther. **14:**37–44.
30. **Samulski, R. J., L. S. Chang, and T. Shenk.** 1987. A recombinant plasmid from which an infectious adeno-associated virus genome can be excised in vitro and its use to study viral replication. J. Virol. **61:**3096–3101.
31. **Sanlioglu, S., P. Benson, and J. F. Engelhardt.** 2000. Loss of ATM function enhances recombinant adeno-associated virus transduction and integration through pathways similar to UV irradiation. Virology **268:**68–78.
32. **Sanlioglu, S., D. Duan, and J. F. Engelhardt.** 1999. Two independent molecular pathways for recombinant adeno-associated virus genome conversion occur after UV-C and E4orf6 augmentation of transduction. Hum. Gene Ther. **10:**591–602.
33. **Schnepp, B. C., K. R. Clark, D. L. Klemanski, C. A. Pacak, and P. R. Johnson.** 2003. Genetic fate of recombinant adeno-associated virus vector genomes in muscle. J. Virol. **77:**3495–3504.
34. **Song, S., P. J. Laipis, K. I. Berns, and T. R. Flotte.** 2001. Effect of DNA-dependent protein kinase on the molecular fate of the rAAV2 genome in skeletal muscle. Proc. Natl. Acad. Sci. USA **98:**4084–4088.
35. **Sun, L., J. Li, and X. Xiao.** 2000. Overcoming adeno-associated virus vector size limitation through viral DNA heterodimerization. Nat. Med. **6:**599–602.
36. **Wagner, J. A., A. H. Messner, M. L. Moran, R. Daifuku, K. Kouyama, J. K. Desch, S. Manley, A. M. Norbash, C. K. Conrad, S. Friborg, T. Reynolds, W. B. Guggino, R. B. Moss, B. J. Carter, J. J. Wine, T. R. Flotte, and P. Gardner.** 1999. Safety and biological efficacy of an adeno-associated virus vector-cystic fibrosis transmembrane regulator (AAV-CFTR) in the cystic fibrosis maxillary sinus. Laryngoscope **109:**266–274.
37. **Wagner, J. A., M. L. Moran, A. H. Messner, R. Daifuku, C. K. Conrad, T. Reynolds, W. B. Guggino, R. B. Moss, B. J. Carter, J. J. Wine, T. R. Flotte, and P. Gardner.** 1998. A phase I/II study of tgAAV-CF for the treatment of chronic sinusitis in patients with cystic fibrosis. Hum. Gene Ther. **9:**889–909.
38. **Wang, Z., H. I. Ma, J. Li, L. Sun, J. Zhang, and X. Xiao.** 2003. Rapid and highly efficient transduction by double-stranded adeno-associated virus vectors in vitro and in vivo. Gene Ther. **10:**2105–2111.
39. **Wu, P., W. Xiao, T. Conlon, J. Hughes, M. Agbandje-McKenna, T. Ferkol, T. Flotte, and N. Muzyczka.** 2000. Mutational analysis of the adeno-associated virus type 2 (AAV2) capsid gene and construction of AAV2 vectors with altered tropism. J. Virol. **74:**8635–8647.
40. **Yan, Z., T. C. Ritchie, D. Duan, and J. F. Engelhardt.** 2002. Recombinant AAV-mediated gene delivery using dual vector heterodimerization. Methods Enzymol. **346:**334–357.
41. **Yan, Z., R. Zak, G. W. Luxton, T. C. Ritchie, U. Bantel-Schaal, and J. F. Engelhardt.** 2002. Ubiquitination of both adeno-associated virus type 2 and 5 capsid proteins affects the transduction efficiency of recombinant vectors. J. Virol. **76:**2043–2053.
42. **Yan, Z., R. Zak, Y. Zhang, W. Ding, S. Godwin, K. Munson, R. Peluso, and J. F. Engelhardt.** 2004. Distinct classes of proteasome-modulating agents cooperatively augment recombinant adeno-associated virus type 2- and type 5-mediated transduction from the apical surfaces of human airway epithelia. J. Virol. **78:**2863–2874.
43. **Yan, Z., Y. Zhang, D. Duan, and J. F. Engelhardt.** 2000. From the Cover: Trans-splicing vectors expand the utility of adeno-associated virus for gene therapy. Proc. Natl. Acad. Sci. USA **97:**6716–6721.
44. **Yang, J., W. Zhou, Y. Zhang, T. Zidon, T. Ritchie, and J. F. Engelhardt.** 1999. Concatemerization of Adeno-associated Viral Circular Genomes Occurs Through Intermolecular Recombination. J. Virol. **73:**9468–9477.